Journal of Alloys and Compounds 938 (2023) 168528

Contents lists available at ScienceDirect

Journal of Alloys and Compounds

journal homepage: www.elsevier.com/locate/jalcom

A review on thermal stability of nanostructured materials

Ningning Liang, Yonghao Zhao *

Nano and Heterogeneous Materials Center, School of Materials Science and Engineering, Nanjing University of Science and Technology, Nanjing 210094, China

ARTICLE INFO

Article history:
Received 29 October 2022
Received in revised form 14 December 2022
Accepted 16 December 2022
Available online 17 December 2022

Keywords:
Thermal stability
Kinetic
Thermodynamic
Nanostructured materials
Microstructural architecture

ABSTRACT

Nanostructured materials, with average grain size in nanometer scale and a high volume fraction of grain boundaries, were known to have advanced mechanical properties, such as high strength, high wear resistance and so on. However, the low thermal and mechanical stabilities have become an important issue to block their practical applications. This paper first reviewed the thermal stability of nanostructured materials, then reviewed the kinetic and thermodynamic strategies for enhancing thermal stability of nanostructured materials as well as their synergy effect. Especially the kinetic approach can stabilize the nanostructure to higher temperatures. The microstructural architecture induced thermal stability was finally reviewed and the generation mechanisms was discussed in point of atomic experiments and perception. Outlook on thermal stability of nanostructured materials was also addressed at the end of paper.

Contents

1. Introduction – significance of nanostructured materials with high thermal stability

Highlights on nanostructured (NS) materials combing with unique characteristic features have indeed renovated the traditional cognitions of structure relating properties. Exhilaratingly, NS materials exhibit dramatic properties such as high strength [1–4], high fatigue and wear resistance [5–7], which always broken the limit of conventional materials rendering attractive applications in industrial and functional fields.

Thermal stability is the ability of materials to withstand temperature changes without microstructural or property performance failure. For structural metallic materials, thermal stability is one of the essential standard in evaluating the service capability, resisting structural failure induced by high temperature [8]. The

* Corresponding author.
E-mail address: yhZhao@njust.edu.cn (Y. Zhao).

https://doi.org/10.1016/j.jallcom.2022.168528
0925-8388/

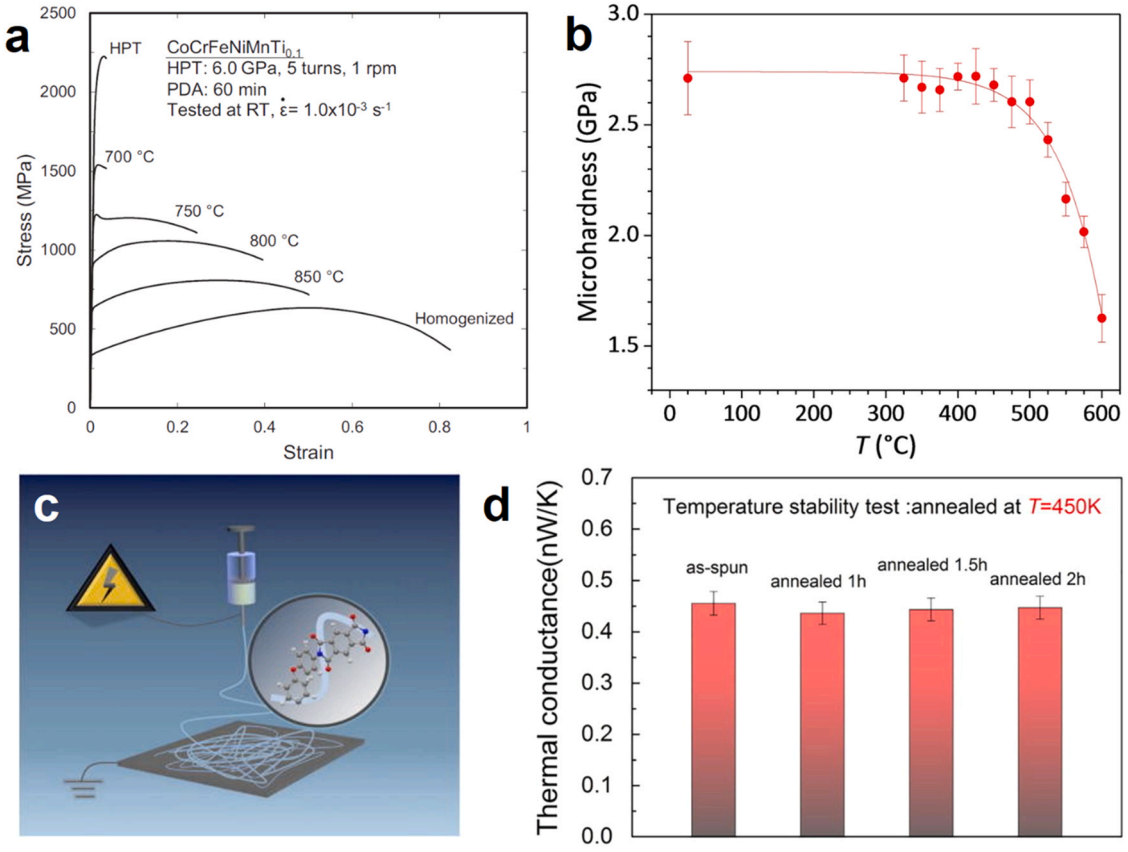

Fig. 1. NS materials with exceptional thermal stability. (a) Engineering stress-strain curves of HPT processed and post-annealed CoCrFeNiMnTi HEA [13]. (b) Variation of surface micro-hardness of the SMRT treated interstitial-free steel with annealing temperature [14]. (c) The electrospinning setup of nanofibers, (d) High-temperature thermal stability test for a PMDA/ODA nanofiber [15].

microstructural thermal stability of ultrafine-grained (UFG)/NS materials is extremely vital for its application and expansion in industrial production [9], especially in the occasion of sustaining high temperature and pressure [10], irradiation and other harsh environment [11,12]. Consequently, stable microstructure is the basic reliable performance and the study of the thermal stability of NS materials has extremely utility value.

For metallic materials with high thermal stability, NS materials can maintain the exceptional mechanical properties at elevated temperatures which were established in high entropy alloys (HEAs) [13,16–22], multilayer materials [23–25], NS pure Cu and Cu alloys [26–30], NS steel [14,31,32], Al alloys [33–35], Ni alloys [36,37] and Mg alloys [38] et al. For instance, the ultimate tensile strength (UTS) of a nano-grained (NG) CoCrFeNiMnTi0.1 HEA deformed by high-pressure torsion (HPT) maintained 1.06 GPa when annealed at 800 °C for 1 h [13], shown in Fig. 1a. Nanolaminated surface layer of an interstitial-free steel processed by surface mechanical rolling treatment (SMRT) kept almost a constant hardness of 2.5 GPa with increasing temperature up to 500 °C for 2 h (Fig. 1b) [14]. The high thermal-stabilized strength promoted the NS materials to be use in the fields of automotive, electronics and aerospace, such as high-speed rail contact line, vacuum pump rotors and electric transformers.

For non-metallic NS materials, in the fields of lithium-ion batteries [39], fibers [15] and nanocomposite [40], high thermal stability was emphasized to implement the stable and safe service performance. For example, as displayed in Figs. 1c and 1d, pyromellitic dianhydride (PMDA)/ diaminodiphenyl ether (ODA) nanofibers which are fabricated by the typical electrospinning posse high-temperature thermal stability up to T = 450 K [15]. Meanwhile, superior thermal conductivity was also detected for the nanofibers facilitating potential candidate for heat dissipation in microelectronic devices.

Herein, this review is expected to be helpful in addressing the historical origin and developing new strategies to obtain thermally stable NS materials. The progress in experiments, approaches and theoretical modeling that have been implemented to stabilize NS materials within the framework of thermodynamics, kinetics and the synergy effect for recent 10 years was reviewed. With the growing interest in the thermo-stable microstructural architecture of NS materials, investigations on the low-energy interfaces, schwarz crystals (SCs) and grain boundary (GB) relaxation are also elaborated. Specially, the summarization and update of representative review articles and their foci is presented in Table 1 as firstly developed by Peng et al. [41–46].

This paper is organized as follows. First, the inherent problems and challenges induced thermos-instability of NS materials are presented in the section'Thermal instability of NS materials'. Second, within the framework of thermodynamics and kinetics, the theoretical models and experimental strategies are reviewed in the section 'Stabilization of NS materials by elements alloying' including 'Kinetic stabilization', 'Thermodynamic stabilization' as well as 'Synergy of kinetic and thermodynamic stabilization'. Third, microstructural construction can be employed to improve the thermal stability by structural restrictions is reviewed in the section of 'Stabilization of NS materials by microstructural architecture'. Finally, the authors summarized this review and proposed several issues that require future systemic investigations in the section 'Conclusions and outlook'.

Table 1
Representative review of literature on thermal stability of NS materials that published in the recent two decades and their foci.

Authors	Year	Title and focus
Andrievski[42]	2003	Title: Review Stability of nanostructured materials Foci: This review focuses on grain growth behaviors of NC materials. The thermodynamic and kinetic factors that influence grain coarsening are briefly analysed. In addition, the'locking' of grain growth due to the 'injection' of vacancies into grain interiors is discussed.
Koch et al.[43]	2008	Title: Stabilization of NC grain sizes by solute additions Foci: Grain growth behaviors of pure NC metals are presented. Strategies of thermodynamic and kinetic stabilizations are independently elucidated. Experimental examples of kinetic stabilization, including reduction of GB mobility, solute drag, second-phase pinning, chemical ordering and grain size stabilization, and thermodynamic stabilization are briefly reviewed
Koch et al.[44]	2013	Title: High-temperature stabilization of NC grain size: Thermodynamic versus kinetic strategies Foci: Strategies of thermodynamic and kinetic stabilizations of NC materials are reviewed. Data of the maximum homologous thermal stability temperatures attained by thermodynamic and kinetic stabilizations are compared and analysed. The role of a kinetic stabilization strategy (Zener pinning) in stabilizing nanostructures at high temperatures is highlighted.
Andrievski[45]	2014	Title: Review of thermal stability of nanomaterials Foci: Thermodynamic and kinetic approaches for stabilizing NC materials are reviewed. Special attention is given to the recent progress in theoretical models that describe the thermodynamics of NC substitutional alloy systems. In addition, experimental research on abnormal grain growth is reviewed
Saber et al.[46]	2015	Title: Thermodynamic Grain Size stabilization models: An Overview Foci: The models of thermodynamic stabilization of binary and ternary alloy systems are reviewed. Two nanostructure stability maps of solute selection for stabilizing NC materials are compared. Additionally, the reduction of GB energy by solute segregation validated by computer simulations is briefly reviewed.
Peng et al.[41]	2017	Title : Thermal stability of nanocrystalline materials: thermodynamics and kinetics Foci : Fundamentals of grain size stabilization by different approaches. First, the stabilizing approaches, thermodynamic stabilization and kinetic stabilization. Second, within the framework of thermodynamics and kinetics, the progress in theoretical models, experiments, and computer simulations is comprehensively reviewed. Third, strategies that are proposed to stabilise the grain size are summarised and discussed

2. Thermal instability of NS materials

2.1. Grain coarsening of pure NS materials

In terms of microstructural evolution, the thermal stability of a NS material is the ability of the NS structure to resist an apparent defects recovery and grain coarsening at elevated temperatures.

For coarse-grained (CG) materials, only a small fraction of atoms spatially located at or in the immediate vicinity of GBs. However, NS materials have a large volume fraction of GBs, leading to more atoms residing near GBs [47,48]. Comparing with grain interior, the atomic packing at thermodynamic non-equilibrium GBs is less dense and more disordered, which increases the configurational and vibrational entropy of the entire system [49] and consequently leads to higher Gibbs energy. This in turn leads to thermal-instability of NS materials where always been performed as restoration process of a micro/nano-structure [42,50,51].

Grain coarsening of NS materials has been frequently observed even at low temperatures [53–56]. NS pure Cu prepared by evaporation exhibits abnormal grain growth at ambient temperature [53]. Huang et al. [54] also reported self-annealing for high purity Cu at room temperature processed by HPT. Lu summarized the variation of grain-coarsening temperature with grain size of several pure metals shown in Fig. 2 [52]. It can observed that grain-coarsening temperature decreases significantly with decreasing grain size. As the grain size is close to 10 nm, the grain-coarsening temperature becomes as low as 0.15 T_m, where T_m is the equilibrium bulk melting point. The inferior thermal stability complicates the processing and limits the potential large scale commercialization of NG pure metals.

Theoretically, the effective driving force P_0 and velocity V_G of thermally driven grain growth on GBs is given in accordance with the Gibbs–Thomson equation by [48,57]:

$$P_0 = \frac{C\gamma_{GB}}{r} \tag{1}$$

C is a numerical constant of order 1, γ_{GB} is the grain-boundary free energy (hereafter referred to as GB energy) and r is the radius of curvature, which is proportional to the grain size, D.

$$V_G = M_{GB}P_0 = M_0\exp[\frac{-Q_m}{RT}]\frac{C\gamma_{GB}}{r} \tag{2}$$

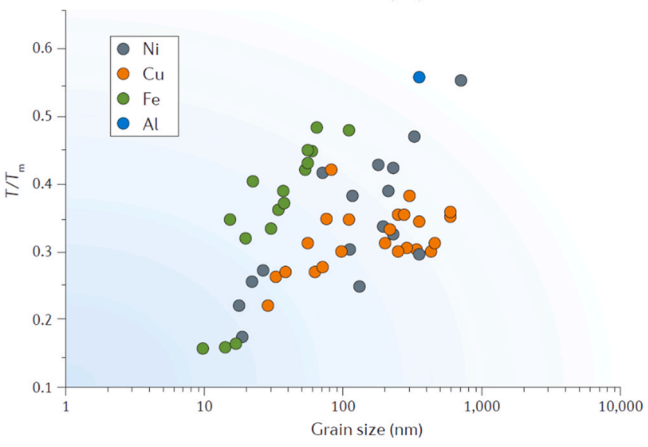

Fig. 2. Reduced temperature for grain coarsening (T/T_m, where T_m is the bulk equilibrium melting point) for the pure Ni, Cu, Fe and Al [52].

M_{GB} is the GB mobility, Q_m is the activation energy and R and T are the gas constant and absolute temperature, respectively. For NS and UFG material, P_0 will be very large as the grain size is reduced to the nanocrystalline size scale (< 100 nm). Meanwhile, plenty of stored enthalpy introduced by dislocation defects as well as high γ_{GB} provide a high driving force and velocity for grain coarsening.

2.2. Thermal instability and mechanical properties of NS materials

With notable microstructure coarsening of NS materials at relative high temperature, the unique mechanical properties at ambient temperature significantly decreased where thermal induced mechanical instability occurred. The decreased strength was owing to grown grains evaluated in Hall-Petch relationship as well as the dissolution of segregation at GBs. For instance, Zhang et al. [58] found that the micro-hardness of HPTed NS 4 N Ni decreased from 300 to 140 HV at low temperatures form 140–180 °C (Fig. 3a) and the narrow temperature interval of 40 °C indicates rapid recrystallization and grain coarsening. NS Al–Ni–Ce alloy was synthesized by sputter deposition [59]. The nano-indentation strength drops considerably from 1350 to 230 MPa when testing temperature increased

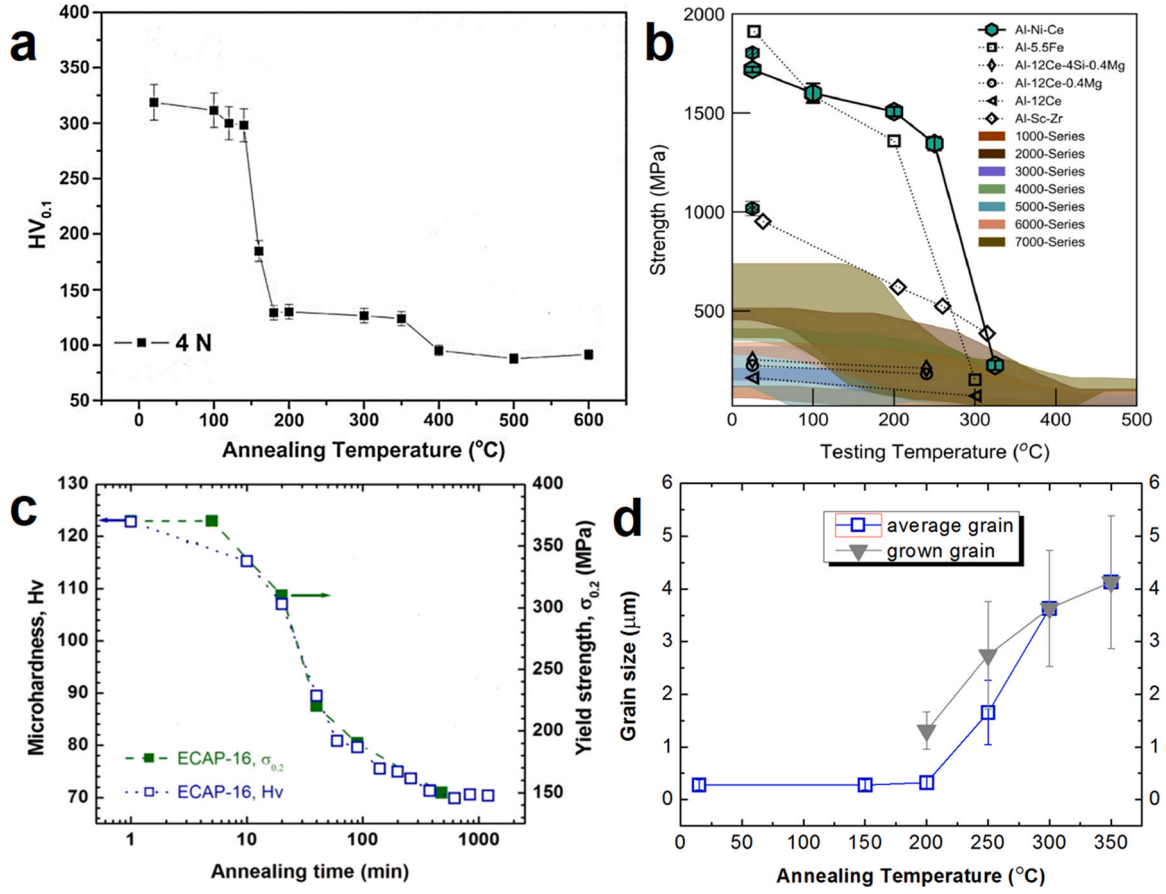

Fig. 3. (a) Hardness as a function of annealing temperature (isochronal annealing for 1 h) of 4 N HPT Ni [58]. (b) Elevated temperature mechanical properties of the Al–Ni–Ce alloy, alongside conventional (1XXX–7XXX series) alloys, Sc and Ce containing alloys, and other high performance Al-alloys [59]. (c) Evolutions of micro-hardness and yield strength of ECAPed 16-passes pure Cu with isothermal annealing time at 200 °C, (d) Average grain size and recrystallized grain size of ECAPed 16-pass pure Cu samples during isochronal annealing for 0.5 h [30].

from 250° to 325°C shown in Fig. 3b, as well as other Al alloys. This is due to significant microstructural coarsening and intermetallic precipitation.

Poor thermal stability of equal channel angular pressing (ECAP) processed UFG Cu has been reported in [30,60–62]. The microhardness and yield strength of ECAPed Cu with 16 passes decreased within minor annealed time and temperatures (Fig. 3c). From thermodynamics point of view, the instability is attributed to the combination of high stored energy and low apparent activation energy for recrystallization [30]. With the increase of ECAP passes, the accumulated strain of dislocation storage improved and increased stored energy [30,63]. The growing fraction of high angle grain boundaries (HAGB) lead to increased nucleation conditions which decrease the apparent activation energy [62]. From kinetics point of view, attributing to the absence of impediment of GB movement (solute segregation, second phase particles, etc.), literature survey indicates that the activation energy of UFG Cu for grain growth should be lower [30,43,62], resulting in early onset temperatures of grain coarsening shown in Fig. 3d.

3. Stabilization of NS materials by elements alloying

In order to improve the thermal stability, alloying elements were always introduced in pure materials as microstructural stabilizer deriving from kinetic and thermodynamic mechanisms [43]. Thermodynamically, lowering GB energy can reduce the driving force for grain coarsening. This is often achieved by solute segregation at GBs, such as in Ni-W [37,64] and Ni-Fe alloys [65]. Kinetically, the driving force for grain coarsening could be counteracted by solute dragging and second phase pinning, introducing impediment of GBs. This is normally achieved by mechanical alloying, such as in Cu-W [66] and Cu-Al alloys [67]. The stability of nanostructure can be further enhanced when thermodynamic and kinetic strategies are favorably combined together. Table 2 summarized the mechanisms of experimental thermal stabilization strategies where kinetics (*K*), thermodynamics (*T*) and both synergy presented (*K*+ *T*), where the quantitative proportion is 53%, 17% and 30%, respectively. It can be seen that most research employed the kinetic or kinetic combining thermodynamic synergy approach for stabilization, and relatively few work focused on the independent thermodynamic strategies.

3.1. Kinetic stabilization

In the kinetic stabilization of NS materials, the GB mobility is reduced by various kinetic mechanisms, such as porosity drag, second phase drag, solute drag, Zener pinning, and chemical ordering [43]. The stabilization of boundary structure due to particle pinning has been widely observed in experiments, for example second-phase and intermetallic particles. The best-known traditional kinetic approach is the containment of grain growth by particles, or the so-called Zener pinning [45]. Classical Zener pinning dominates this mechanism and can stabilize the grain size of the NS materials to relative higher temperatures. In the following, the theory and experiments results of Zener pinning stabilization is expounded from the perspective of kinetic mechanisms.

Table 2
Mechanisms of experimental thermal stabilization strategies, including kinetics (*K*), thermodynamics (*T*) and both synergy presented (*K+T*).

Sample	Strategies	Sample	Strategies
UFG Al-Fe alloy[33]	*K*	NS carbon-containing FeMnCoCrNi iHEA[68]	*K*
NS Al-Zr alloy[34]	*K*	UFG Ni alloys[69]	*T*
NS CoCrFeMnNi alloy[13]	*K*	NS Ag-W alloys[70]	*T*
NS Mg-Gd-Y-Zr alloy[38]	*K*	NS Cu-Zr-Hf alloys[71]	*T*
UFG CoCrFeNiNb HEA[19]	*K*	NS Mg–Ti alloy[72]	*T*
UFG Mg-Zn-Ca-Zr alloy[73]	*K*	NS Mg alloys[74]	*T*
UFG Fe–22Mn–0.6 C steel[31]	*K*	NS Ni-W alloy[64]	*T*
UFG Cu matrix[75]	*K*	UFG Mg-Gd-Y-Ag-Zr alloy[76]	*T*
NS Cu-Al alloy[67]	*K*	NS Ni-Fe alloy[65]	*T*
NS Ni-Mo alloy[36]	*K*	NS austenitic stainless steel[12]	*T+K*
NS Fe composites[77]	*K*	NS Cu-Ag/Fe triphase multilayers[78]	*T+K*
NS Mg-Al-Zn-Ti alloy[79]	*K*	UFG Cu-Cr-Zr alloy[80]	*T+K*
NS Cu-W alloy[66]	*K*	UFG Al–7Mg alloy[81]	*T+K*
UFG Al-Cu alloy[82]	*K*	UFG ECAPed Cu-Cr-Zr alloy[26]	*T+K*
NS Al-5083 alloy[83]	*K*	NS Fe-18Cr-8Ni stainless steel[84]	*T+K*
NS CoCrFeNi HEA[20]	*K*	NS Al-Mg alloy[85]	*T+K*
NS Fe-Zr alloy[86]	*K*	NS NbMoTaW HEA[87]	*T+K*
NS NiTiWx thin films[88]	*K*	NS Pt-AuPd alloy[89]	*T+K*
NS Ni-W alloy[37]	*K*	NS Ti6Al4V5Cu alloy[90]	*T+K*
NS Fe-Zr steel[91]	*K*	NS Ta-Hf multilayer[92]	*T+K*
NS Ni-SiOC amorphous ceramic reinforced metals[93]	*K*	NS Al-Fe-Ti alloys[94]	*T+K*
Cu alloying UFG Fe–22Mn–0.6 C steel[95]	*K*	NS Ni–ZrNbMoTa alloy[96]	*T+K*
UFG 9Cr-ODS steel[97]	*K*	NS Ni-containing HEA[22]	*T+K*
NS Al-Ni and Al-V alloys[98]	*K*		

It is well known that the presence of second-phase particles in a polycrystalline material can limit grain growth by pinning their boundaries [83]. Generally, two processes that emphasized by Hanna et al. [83] are in accountable for particle pinning. In the first process, incoherent particles tend to accumulate at the boundaries because they reduce their areas and hence the energy of the system. In the second process, a boundary motion is hindered since its migration has this requirement: the creation of more boundary area, where particles previously resided. As a result, an increase in the energy of the system will be essential. The above two processes are the basis of the idea originally proposed by Zener in a communication to Smith [99]. The pinning force between a single particle with the radius r and a boundary could be given by [83]:

$$p_i = \pi r \gamma_{GB} \tag{3}$$

In a system in which the area density of the disperse particles is:

$$n_p = \frac{3f_{particle}}{2\pi r^2} \tag{4}$$

where f_{particle} is the volume fraction of pinning particles, for the case in which many particles interact with the boundary, the total pinning force was given to:

$$P_z = n_p \cdot p_i = \frac{3f_{particle}\gamma_{GB}}{2r} \tag{5}$$

Eq. (5) is the well-known form of the Zener pinning force on the GBs [79,99]. Based on Zener's development reported elsewhere [100,101], the driving force, F_D, for grain growth may be given by:

$$F_D = 2\gamma_{GB}/D \tag{6}$$

When the system is in equilibrium, $P_Z = F_D$. Under this condition, the critical average grain size, D_c, related to Zener effect can be obtained by the following equation:

$$D_c = \frac{4cr}{3f_{particle}} \tag{7}$$

where c is a constant. The above equations implied that precipitates of smaller size and large volume fraction are much more effective in pinning the GBs by Eq. (5) and resulting in smaller annealed grains in Eq. (7) [67,75,102]. Hanna et al. [83] predicted the D_c value of 33 nm of Al 5083 alloy pinned by diamantane nanoparticles. This estimation is in good agreement with experiment observations suggesting that Zener GB pinning i.e. kinetic grain size stabilization is the key strengthening mechanism during high-temperature annealing.

Experimentally, Zener pinning was widely adopted to impede microstructure coarsening. Gao et al. [95] introduced minor Cu alloying into UFG structures in a typical Fe–22Mn–0.6 C steel and the thermal stability was notably enhanced to 910 °C for 5 min and 760 °C for 60 min annealing (Fig. 4a). Owing to the rapid and copious precipitation, Zener pinning pressure P_z increases rapidly and exceeds the driving force for grain growth P_g throughout 20 min annealing (Fig. 4b), suggesting that these freshly recrystallized submicro grains are persistently stabilized. The copious Cu-rich nanoprecipitation is responsible for the pinning of GB migration shown in Fig. 4c. Chakravarty et al. [67] reported the precipitation of nanoscale Cu-Al intermetallic phases (mainly $CuAl_2$ and Cu_9Al_4) stabilize the nanocrystalline grain size to high homologues temperature ~0.87 T_m in Cu-12 at% Al alloy. High density nano-sized precipitates in HP-Thermal-Compression produced Fe-5 at% Zr steel retained the grain size of 30 nm at 923 K and 250 MPa contributing the excellent creep resistance [91]. In heat treatable UFG Al-4.5%Cu alloy shown in Fig. 5, nano-particles have precipitated in the GBs (Fig. 5b to d) thereby retarding the grain growth process and inducing conspicuous microstructural stabilization to 350 °C(Fig. 5a) [35].

The pinning effect was also performed together with some other mechanisms such as solute segregation [34], twinning [75] and nanoclusters drag [86]. AlZr precipitates was produced in HPT deformed nanocrystalline Al-5%Zr alloy after aging. The precipitates and Zr segregations suppress GB migration by pinning and provide a remarkable thermal stability [34]. The thermal energy during annealing (0.55 T_m) does not provide enough driving force for grain growth due to the restriction by micro-particles and TBs in UFG Cu/CrB and Cu/CrB_2 samples [75].

Another form of Kinetic stabilization is depicted by sluggish diffusion. Especially in HEA, the lack of a major diffusion element and a huge discrepancy of atoms size also weighted in favor of

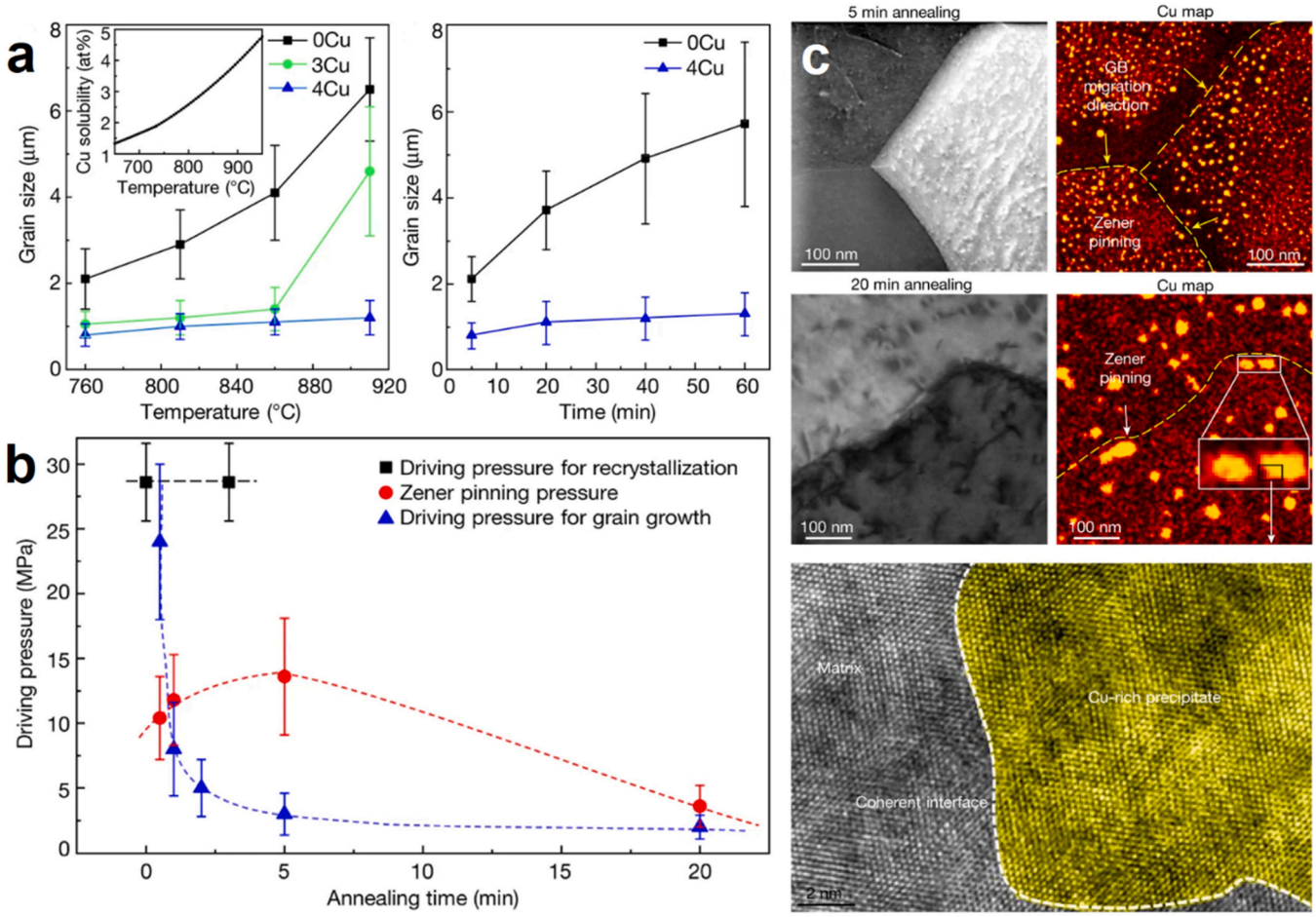

Fig. 4. (a) Effects of annealing temperature and time on the UFG structure. Evolution of the grain size of 0Cu, 3Cu and 4Cu after annealing at 760, 810, 860 and 910 °C for 5 min and evolution of the grain size of 0Cu and 4Cu as a function of the annealing time (from 5 min to 60 min) at 760 °C. 4Cu exhibits the most stable UFG structure, (b) Evolution of driving pressure for recrystallization, driving pressure for grain growth and Zener pinning pressure as a function of annealing time, (c) Annular bright-field scanning transmission electron microscopy (STEM) images (left) and their corresponding STEM energy-dispersive spectroscopy (EDS)- spectrum images (right) of 4Cu annealed at 760 °C for 5 min and 20 min, demonstrating evidence for Zener pinning. High-resolution TEM (HRTEM) image of one nano-precipitate (NP) at a GB showing a coherent interface with the shrinking grain [95].

sluggish diffusion [103,104]. Sluggish diffusion kinetics is an important contributor to the outstanding properties of HEA and a strong resistance against grain coarsening, resulting in slow atom segregation, precipitation and migration process [105,106]. Zhou et al. [22] summarized the mechanisms of sluggish diffusion effect on thermal stability in three ways: (i) local sites with a wider distribution of metastable energy levels, (ii) the slowest diffusion rates of segregating element and (iii) Zener pinning. Jiang et al. [19] designed an ultrafine-lamellar CoCrFeNiNb0.45 eutectic HEA and found that the high thermal stability is contributed by sluggish diffusion effect, and low-energy phase boundaries and near-equilibrium microstructure of eutectic HEAs. NS CoCrFeNi HEA was synthesized by Praveen et al. [20] with mechanical alloying followed by spark plasma sintering. Comparing with normal nanocrystalline metals, sluggish grain growth of nanocrystalline HEA (Fig. 6a) is attributed to the Zener pinning effect from the fine dispersion of oxide, mutual retardation of GBs in the presence of two phases, and sluggish diffusivity because of cooperative diffusion of multi-principle elements. The size of face-centered cubic (FCC) phase, Cr_7C_3 and Cr_2O_3 precipitates remain nearly unchanged controlled by sluggish diffusion in heat treated condition (700 °C for 600 h) in Fig. 6b. Sluggish diffusion effect was also observed in conventional binary alloy by lower diffusion coefficient. For example, the thermal stability of Al-5at%V was higher than that of Al-5at%Ni, which was attributed to the lower diffusion coefficient of V in Al retained a considerably larger amount of V in solid solution even after heat treatment at 400 °C, whereas, the higher diffusivity of Ni leads to the formation of coarse intermetallics in Al-5at%Ni alloys at lower temperatures [98].

3.2. Thermodynamic stabilization

The driving force for grain growth is directly proportional to the GB energy, then the driving force for grain growth will be lowered by reducing the GB energy especially for NS materials with high fraction of GBs, which is elaborated by thermodynamic stabilization. The thermodynamic mechanism has proven to be successful in overcoming the intrinsic instability of NS materials. The thermodynamic approach depends on introducing solutes that segregate to the GBs such that the free energy of the system reaches a local minimum impeding grain growth. This concept has been frequently modeled and experimented as reviewed in the following.

Several researches has modeled and calculated the thermodynamic reduction of GB energy by solute segregation, methodical design-based approach for selecting solutes in binary NS alloys and

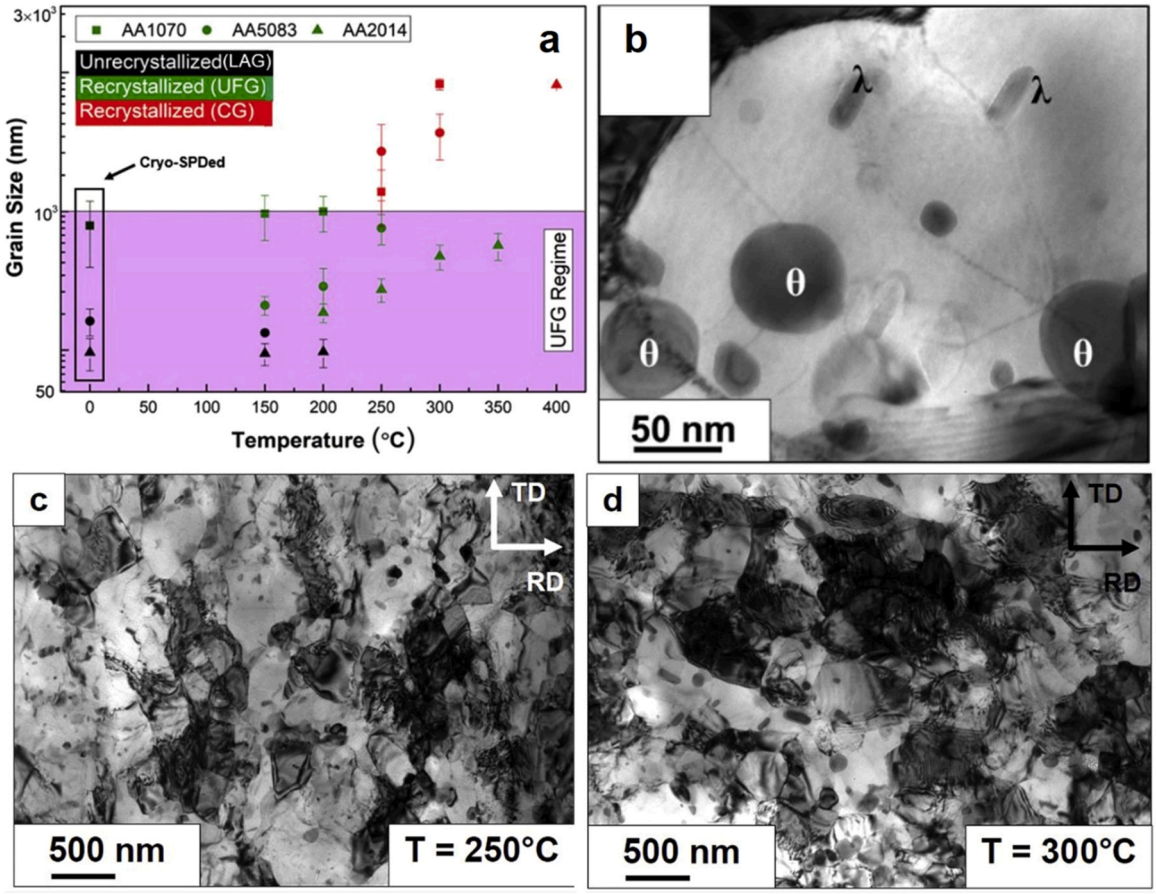

Fig. 5. (a) Variation of grain size with respect to the annealing temperature for pure aluminum and aluminum alloys, (b) TEM images of the λ, θ precipitates formed after annealing of AA2014 alloy at 250 °C, Microstructural evolution during annealing of AA2014 alloy at various annealing temperatures: (c) 250 °C, (d) 300 °C [35].

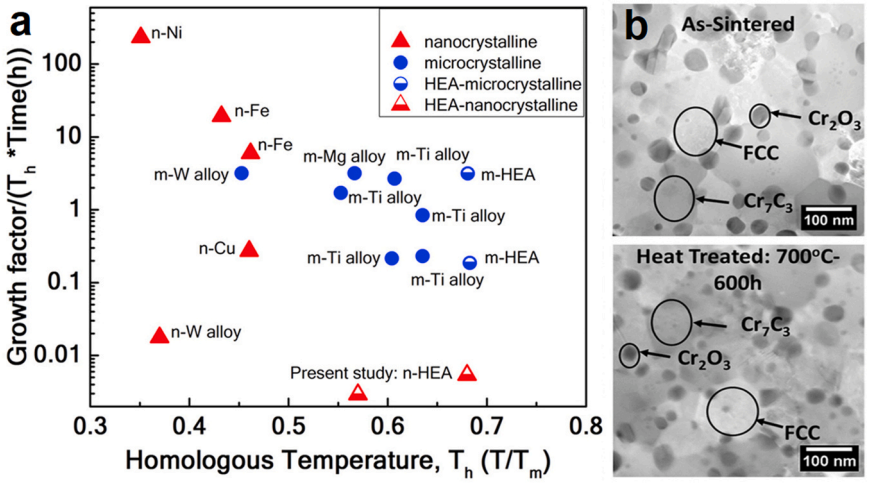

Fig. 6. (a) Normalized grain growth factor Vs homologous temperature summarizing on grain growth, (n indicates nanocrystalline materials, m indicates microcrystalline materials), (b) The STEM image of as-sintered compact and specimen that was heat treated at 700 °C for 600 h, the precipitates remain nearly unchanged [20].

diffuse-interface model of GB segregation in binary metallic alloys by the method of first principles and phase field model [48,107,108]. Since the values of segregation energy (ΔG_{seg}) are usually not available, they are estimated. Wynblatt and Chatain [108,109] reviewed the analytical models on segregation to GBs and surfaces and addressed the difficulty of meaningful definitions of segregation enthalpy, entropy, and free energy among various issues. The central equation for all models is as follows for a binary system:

$$\frac{x_B^{GB}}{1-x_B^{GB}} = \frac{x_B^{I}}{1-x_B^{I}} \exp\left[-\frac{\Delta G_{seg}^{ex}}{RT}\right] \tag{8}$$

where $x_B^{GB}$and x_B^I are the mole fractions or solute concentration of component B (solute) in the GB and grain interior, respectively. ΔG_{seg}^{ex} is the excess Gibbs energy of segregation. Then Zhang et al. [69] calculated the GB energy by solving Gibbs adsorption equation in the dilute limit:

$$\gamma = \gamma_0 + \Gamma_s(\Delta H_{seg} - T\Delta S_{seg}) \tag{9}$$

where γ is surface energy, γ_0 is the interfacial energy of the solvent, Γ_s is the specific solute excess at the interface and assumed as:

$$\Gamma_s = \frac{2(x_B^{GB} - x_B^I)}{\sigma} \tag{10}$$

which is for double monolayer and σ is the molar area of a monolayer. ΔH_{seg} and ΔS_{seg} are the enthalpy and entropy of segregation, respectively, given that $\Delta G_{seg} = \Delta H_{seg} - T\Delta S_{seg}$, rearranging of Eq. (9) gives the normalized GB energy as:

$$\frac{\gamma}{\gamma_0} = 1 + \Gamma_s\frac{\Delta G_{seg}}{\gamma_0} \tag{11}$$

It can be the criterion that, when $\Delta G_{seg} < 0$, solute segregation to the GB is favored and γ decreases. Thermal stability of the alloy is elevated. When $\Delta G_{seg} > 0$, desegregation is favored and γ increases.

Darling et al. [108] and Zhang et al. [69] calculated and found that each γ/γ_0 curve has a minimum value and the GB energy decreases with increasing x_B^{GB} before it reaches the minimum value shown in Fig. 7a. However, the GB energy increases with increasing x_B^{GB} after it reaches the minimum value. The equilibrium condition of the system with respect to grain growth is stipulated by $\Delta G_{seg} = 0$, reaching the saturation of solute concentration at GBs. For Fe-Zr alloy shown in Fig. 7a with the molar Zr fraction x_0 is 0.03 and the temperature is 550 °C, the saturated solute mole fractions in the GB is 0.26 [108]. For Ni alloys shown in Fig. 7b, the saturated solute concentration of $Ni_{99}Fe_1$ and $Ni_{99}Cr_1$ is ~ 1.5 at%, whereas the saturated solute concentration of $Ni_{99}V_1$ and $Ni_{97}Cr_3$ is ~ 4.5 at% [69]. After the solute concentration is saturated at GBs, ΔG_{seg} is positive and continues to increase with increasing solute concentration at GBs, suggesting that more enrichment of solute at GBs is thermodynamically unfavorable. Schuh's group developed theoretical framework with which the GB segregation behavior in ternary alloys can be estimated based on the thermodynamic properties of the constituent binary systems using Monte Carlo simulations and high-throughput combinatorial technique [110–112]. The alloy systems explored computationally are experimentally validated via advanced characterization techniques exploring the stability of binary and ternary nanocrystalline alloys, such as Fe-Mg alloy [113,114], Pt-Au-Pd alloy [89,111].

Experimentally, grain growth can be inhibited by solute segregation and segregation of certain solute atoms to GBs can reduce the GB free energy and thus lower the driving force for grain growth. The thermodynamic strategy exhibits weak temperature dependence and has been extensively studied. Jiao and Schuh [70] studied the effect of W additions on the grain structure, GB segregation, and thermal stability of nanocrystalline Ag-W alloys. As depicted in Fig. 8a, the Ag-W alloys with GB segregation show enhanced stability with no structural changes after annealing for 24 h at 200 °C. The GB segregation enthalpy for W in Ag is calculated to be in the range of 1.7–9.4 kJ mol^{-1} suggesting that W segregation in Ag-W should lower the GB formation energy, providing thermodynamic stability. Slight segregation of Fe and impurities in NS Ni contributed the good thermal stability and annealing hardening was achieved by Zhang et al. [65]. The high volume fraction of GBs in NC grains results in a large fraction of solute and/or impurities accommodated in the GBs, shown in Fig. 8b, consequentially reducing specific GB energy, γ. According to the equation developed by Kirchheim [115], the free energy change in a closed system due to a change in GB area dA, is $dG = \gamma dA$. The reduced γ lowers the thermodynamic driving force for grain growth. In Mg alloys, GB segregation of solute can restrain the grain growth to high temperatures versus room temperature growth of NS Mg-based materials [72]. The segregation of Ti solute at GBs during annealing largely enhanced the thermal stability from 100 °C for NS Mg to 450 °C for Mg-Ti alloy shown in Fig. 8c which was verified by electron energy loss spectroscopy analysis. Xiao et al. [76] produced an Mg-Gd-Y-Ag-Zr alloy having the nanoscale interfacial phases which are better for improving the combination of mechanical property and thermal stability than high density precipitates within grains. When the structure is ordered in coordination with large Gd atoms and small Ag atoms, shown in Fig. 8d, the lattice strain and the number of vacancies can be reduced, leads to a lowered interfacial energy. The low energy nature of the coaxial GB with the interfacial phase leads to higher stability. Thermodynamic effects can also work with thick amorphous inter-

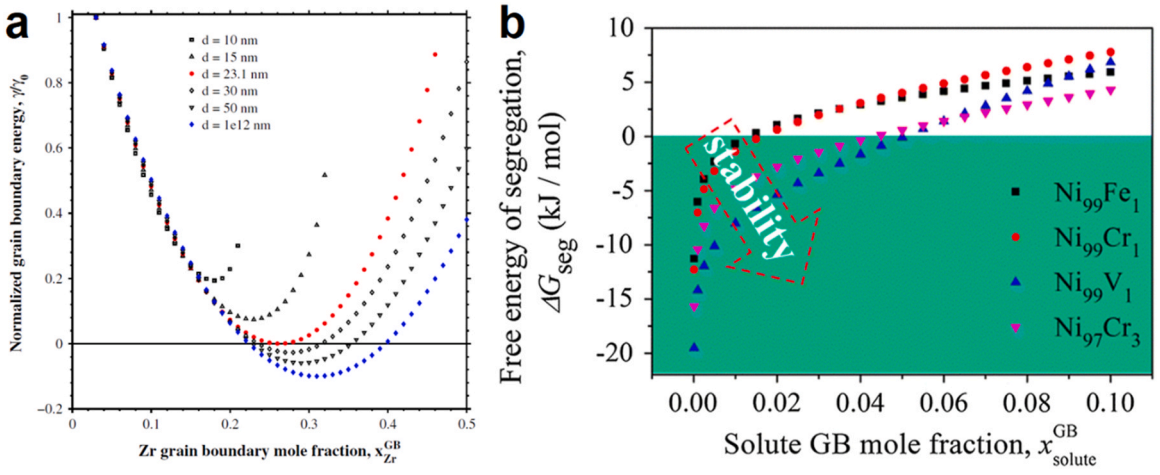

Fig. 7. (a) Normalized GB energy γ/γ_0 versus mol fraction of Zr atoms on the GB for several different grain sizes of Fe-Zr alloys: 10, 15, 23.1, 30, 50 and 1×10^{12} nm [108]. (b) Change in the free energy due to solute segregation, ΔG_{seg}, versus the fraction of solute atoms on the GBs for $Ni_{99}Fe_1$, $Ni_{99}Cr_1$, $Ni_{99}V_1$ and $Ni_{97}Cr_3$ [69].

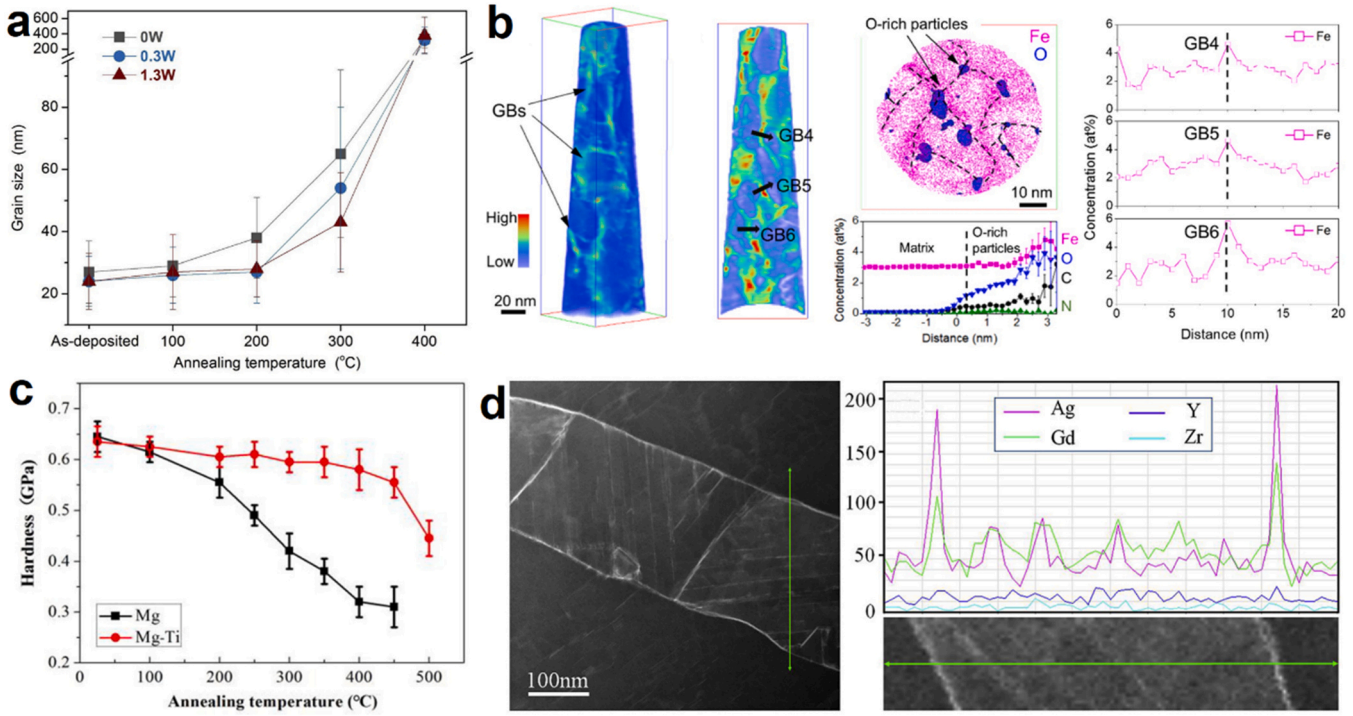

Fig. 8. (a) Average grain sizes of the Ag-0 W, 0.3 W, and 1.3 W alloys as a function of annealing temperature [70]. (b) Line scanning 3D atomic density map of a reconstructed volume of the annealed NC $Ni_{99}Fe_1$ alloy [65]. (c) Microhardness of NC Mg and Mg-Ti as a function of annealing temperature [72]. (d) High angle annular dark field (HAADF)-STEM image of a band structure enclosed by two 142° coaxial GBs and Line scanning EDS [76].

granular films to stabilize NS Cu-4Hf-1Zr alloy reported by Grigorian and Rupert [71] and the grain sizes were retained well within the nanocrystalline regime after annealing for two weeks at a temperature above 95% of the solidus temperature.

3.3. Synergy of kinetic and thermodynamic stabilization

Regarding that both the above independent thermodynamic and the kinetic approach for grain growth contribute to the thermal stability of NS materials, a more stable NS material may be designed, if considering additionally the kinetic stabilization based on the thermodynamic framework, i.e. stabilization strategy of NS materials by consideration of the thermo-kinetic synergy. Peng et al. [116] used first-principles calculations for a series of combinations between fifty-one substitutional alloying atoms as solute atoms and Fe atom as fixed solvent atom, and they found that the thermal stability neither simply increases with increasing the segregation enthalpy as expected by thermodynamic stabilization, nor monotonically increases with increasing the activation energy for bulk diffusion as described by kinetic stabilization. Validity of this thermo-kinetic stabilization criterion has been tested by current experiment results of Fe-Y alloy and previously published data of Fe-Zr [57] alloys.

Complementary thermodynamic and kinetic stabilization approach has been widely reported by simultaneous segregation and pinning. The grain size of as-sputtered Al-10% Mg alloy films (3.3 nm) only increased by 69% to 6.1 nm after annealed at 300 °C for 3 h (Fig. 9a and b) [85]. Coarsening resistance of NS Al-Mg alloys is attributed to a combination of thermodynamic stabilization of GBs by controlled Mg segregation, and kinetic stabilization through pinning of the boundaries with nanoscale intermetallic precipitates. The formation of nanoscale intermetallic precipitates was identified in both the computational predictions and experimental results as shown in Fig. 9c. Du et al. [12] reported an NS austenitic stainless

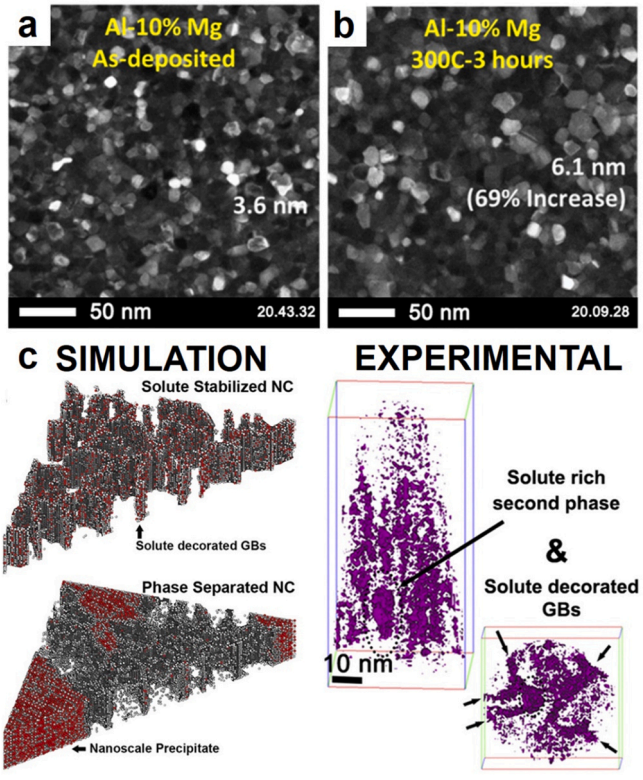

Fig. 9. STEM images of as-sputtered (a) and annealed (b) at 300 °C for 3 h films of Al-10% Mg, (c) Computationally predicted Mg atom distribution in solute stabilized nanocrystalline and the solute stabilized and phase separated nanocrystalline states, correspond to atom probe tomography (APT) results [85].

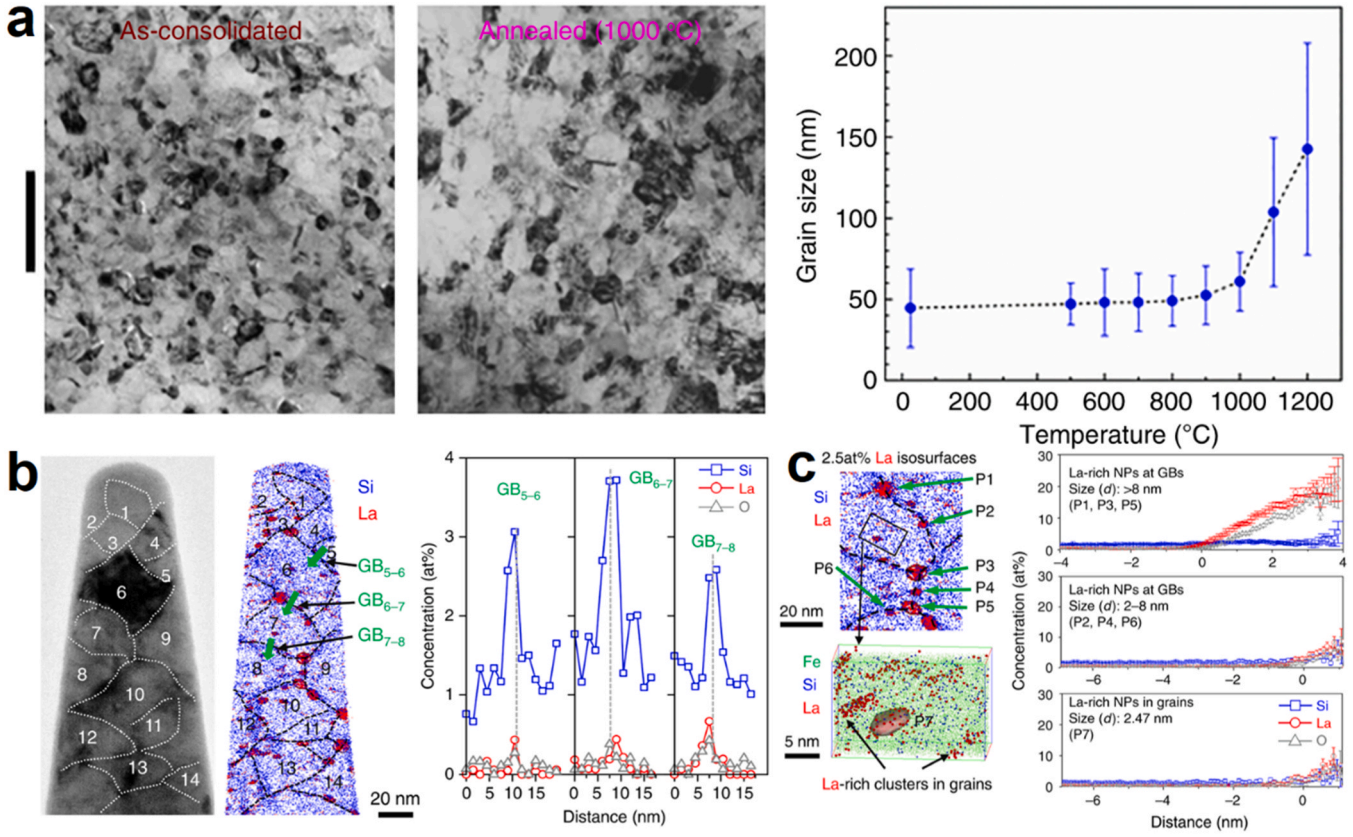

Fig. 10. (a) TEM images of as-consolidated and annealed (at 1000 °C for 1 h) NC-SS. Scale bar, 200 nm, and grain size of as consolidated NC-SS vs. annealing temperature, (b) A bright field TEM image and corresponding APT Si atom map of a thin slice reconstructed volume, with 14 resolved nanograins marked as 1–14, respectively and GBs decorated with La-rich NPs. 1D composition profiles across GB5–6, GB6–7, and GB7–8, as marked by green arrows in the Si map, showing the segregation of Si, La, and O at GBs, (c) A top magnified combined atom map of La from a small reconstructed region with GBs decorated with La-rich NPs, a bottom combined Fe, Si, and La map of a small framed region of a grain containing a La-rich NP defined by iso-surfaces of 2.5 at% La and fine La-rich clusters. The right programs from La-rich NPs in different sizes reveal their compositions of La-rich NPs at GBs and in grain interiors [12].

steel (NS-SS) containing 1 at% lanthanum with an average grain size of 45 nm that exhibits exceptional thermal stability up to 1000 °C (0.75 Tm) as illustrated in Fig. 10a. Some elemental Si, La, O atoms are segregated at GBs and thermodynamically stabilize the nanograins in NC-SS (Fig. 10b). The remained elemental La atoms form a high density of La-rich NPs mainly distributed along GBs and provide additional kinetic resistance against grain growth (Fig. 10c). These two factors play a critical role in accomplishing the outstanding thermal stability of nanograins in NC-SS.

For HEAs, utilize high-entropy GB complexions to enhance the thermal stability of NS alloys at high temperatures. GB energies could be reduced via bulk and/or GB high-entropy effects at/within the solid solubility limit to reduce the thermodynamic driving force for grain growth at high temperatures. Moreover, grain growth can be hindered by the high-entropy sluggish kinetics at GBs. Zhou et al. [22] stabilized a Ni-based $Ni_{80}Mo_{6.6}Ti_6Nb_6Ta_{1.4}$ alloy and a Ni-containing high-entropy $Ni_{25}Fe_{23}Co_{23}Cr_{23}Mo_2Nb_2Zr_2$ alloy up to 1000 °C via an innovative use of high-entropy GB complexions thru both thermodynamic and kinetic effects. A bulk dual-phase AlCoCuNi medium-entropy alloy was prepared by mechanical alloying and could maintain the nanostructures as well as a high hardness of about 580 HV even after annealing at 900 °C for 50 h [8]. The extremely high thermal stability has been attributed to the extensive thermal-stabled low-energy phase boundaries, LAGBs, the high-entropy and sluggish diffusion effects.

Focusing on the comparison of thermodynamic versus kinetic stabilization, the Zener pinning mechanism may provide the best thermal stabilization to higher homologous temperatures as shown in Fig. 11a. As discussed by Koch et al. [44], the solutes will be insoluble in equilibrium and only nonequilibrium processing methods can induce metastable solid solutions. However at sufficiently high annealing temperature, the solutes will come out of solution and segregate to GBs. With the optimum kinetics of nucleation and growth of the second phase, nanoscale phases can be obtained, which may be effective for Zener pinning. At the same time, the solute segregation may induce minor reduction of GB energy or thermodynamic driving force. For example, in electro-deposited NG pure Ni and Ni-Mo alloys, GB energy in the NG Ni-Mo alloys after Mo segregation at GBs, is slightly higher than that in NG pure Ni, insensitive to Mo concentrations shown in Fig. 11b [36]. The enhanced GB stability in the as-annealed NG Ni-Mo alloys is ascribed to GB pinning by Mo atoms rather than GB energy reduction. The above suggestion that kinetically reduced mobility by Zener pinning may be more effective strategy for stabilizing NC materials at higher temperatures than thermodynamic mechanism.

4. Stabilization of NS materials by microstructural architecture

While without alloying treatment, for pure materials, structural stabilization is faced with more challenges due to loss of segregation

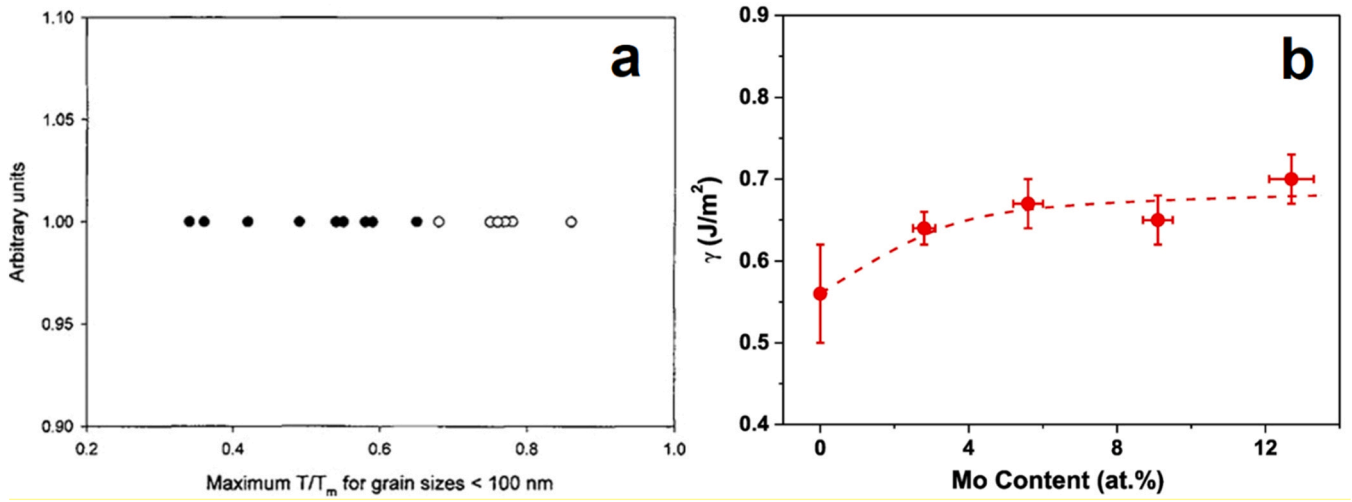

Fig. 11. (a) Maximum homologous temperature (T/T_m) for grain sizes < 100 nm. Possible thermodynamic stabilization (•) and possible Zener pinning (O), data summarized in [44]. (b) Calculated GB energy (γ) for the as-annealed NG Ni and Ni-Mo alloys as a function of Mo content [36].

induced GB pinning and lowing boundary energy mentioned before. Through mechanical process, significantly thermostable microstructure can be manufactured in NS metals by modifying the architectures of their interfaces, such as low-energy interfaces, SCs and related GB relaxtion. By tailoring the structure and distribution of these thermostable architectures, anomalous thermal stability can be achieved for NS materials. Furthermore, in some alloys higher thermal stability can be obtained by multiple mechanisms responding from microstructure artifacts, sluggish diffusion and solute segregation.

4.1. Low-energy interfaces

Low-energy interfaces, such as twins and LAGBs, are born with the extremely low excess enthalpy and weak mobility, and then the thermal stability of these nano-scaled structures in metals is generally superior to those of NG structures [14,30,52,117]. Liu et al. [118] found the 2D nanometer-scale laminated structure on top layer of bulk Ni with low-angle boundaries by surface mechanical grinding treatment (SMGT) is ultra-thermo-stable up to 500 °C annealing for 1 h, comparing with 3D UFG structure shown in Fig. 12a and b. This is attributed to the low excess energy and low mobility of the low-angle boundaries. The authors studied the thermal stability of pure Cu with two different UFG microstructures: one with lamellar grains and LAGBs and another with equiaxed grains and HAGBs [30]. Thermodynamic calculations and kinetic analysis revealed that grain structures with LAGBs possess lower stored energy and higher activation energy relative to HAGBs, resulting in higher thermal stability. Accordingly, it can be seen that the lamellar structure with specific boundaries has the capacity to stabilize structure.

For twins, as shown in Fig. 12c and d, dynamic plastic deformation (DPD) produced nano-twins survived after 300 °C and 400 °C annealing for 10 min in Cu-5Ag alloy, indicating nano-twin bundles exhibit a higher thermal stability against recovery and recrystallization in comparison with that of the NGs [119]. TB possesses much lower excess energy than that of HAGB (for Cu, γ_{TB}=0.02–0.04 J m^{-2}, γ_{GB} = 0.625 J m^{-2}). The total stored energy in the nanotwin bundles is much smaller than that in the NG regions. Dhal et al. [120] also processed UFG grains enriched with deformation nanotwins in severely cryo-rolled Cu. Excellent thermal stability combined with high strength-ductility synergy is observed during isochronous annealing, where nanotwins formed during cryo-rolling are retained upto a high annealing temperature of 300 °C. The authors found that in HPT deformed FeNi2CoMo0.2V0.5 HEA, nanotwins can maintained to as high as 600 °C [106]. TBs reduced the migration rate of GBs, by lowering the overall coarsening rate and the coherent TB is well known to be immobile in response to thermal agitation. Then the high thermal stability of FeNi2CoMo0.2V0.5 HEA is derived from stable twins coacted with sluggish diffusion effect.

4.2. Schwarz crystals

In NG copper with a few nanometers in size, a metastable structure was discovered in which GBs constrained by quadrupolar network of coherent TBs resemble essentially the triply periodic minimal surface (TPMS) of Schwarz primitive diamond (D), as illustrated in Fig. 13a. The extremely fine-grained structures with GB or interfacial morphologies featured by any topological manifold of minimal surface, called Schwarz crystal, represent a novel type of intrinsic metastable state in polycrystalline metals at an ultimate grain size limit [121,122].

The SCs are found to exhibit superior thermal and mechanical stabilities than any other forms of metastable solid states known so far, for example, the metallic glasses. Li et al. [121] use a two-step plastic deformation process of SMGT followed by HPT in liquid nitrogen to produce the SC, which is formed by the evolution of GBs into three-dimensional (3D) minimal interface structures constrained by TB networks. In this type of polycrystal, annealing induced grain coarsening is effectively suppressed, and the 10 nm grain size was remained even close to the melting point (1348 K), shown in Fig. 13b to d. In Al-15%Mg alloys, SC was also observed in sample processed by HPT at 77 K under a hydrostatic pressure of 10 GPa, and the applied strain exceeded 20 [123]. The SC structure possess inherent diffusionless feature and seems to provide a robust barrier for arresting the diffusion of atoms in metals and substitutional alloys, boosting stability up to melting temperatures. This stability is much higher than that for conventional alloys.

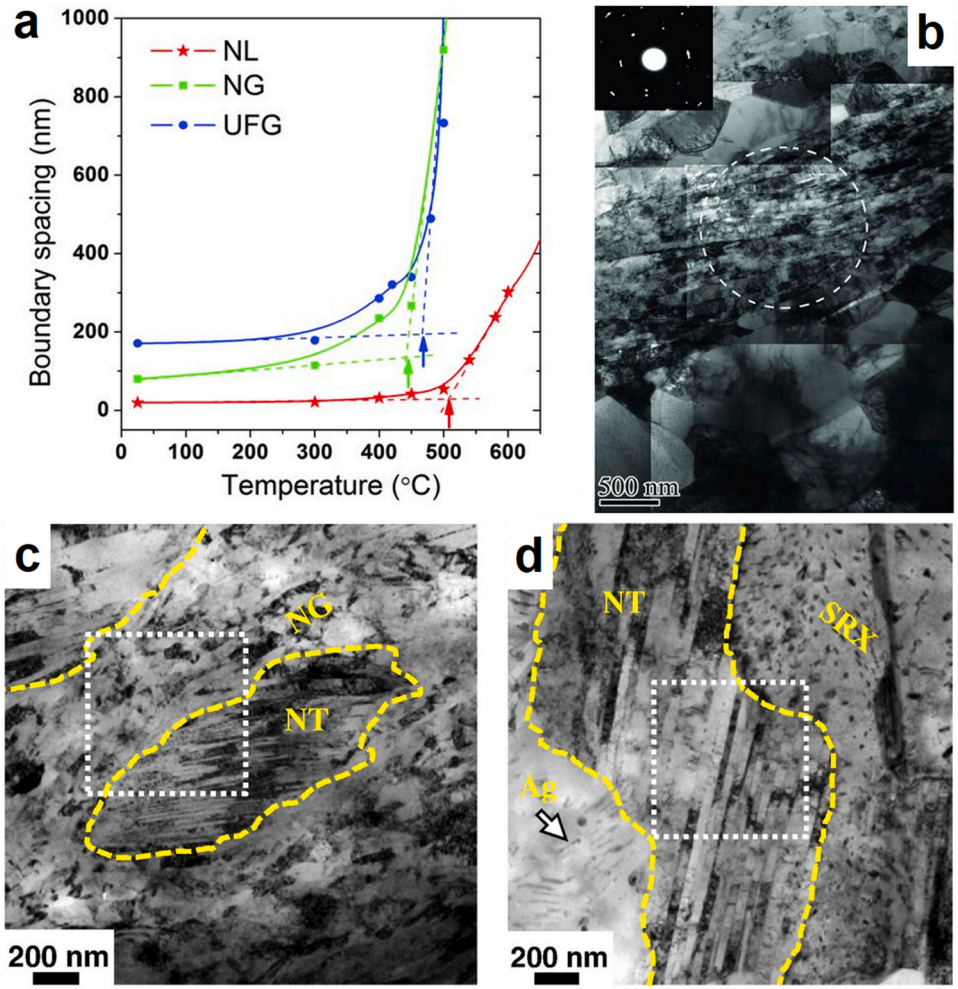

Fig. 12. Thermal stability of the low-energy interfaces. (a) Variations of boundary spacing of the UFG, NG, and nanometer-thick laminated (NL) structures as a function of annealing temperature (for 1 h), (b) A bright-field TEM image of the alternative NG/NL structures in the SMGT Ni sample after annealing at 500 °C for 1 h [118]. Bright-field TEM morphology of DPD samples after annealing at (c) 300 °C and (d) 400 °C for 10 min [119].

Jin et al. [122] addressed the constraining effects of 3D coherent TB (CTB) network on the formation and thermos-stability of SC via atomistic simulations. It was shown that GB migration and evolution of CTB network trigger formation of SC diamond. CTB constraints are critical to generate GBs of zero mean curvature underlying vanishing capillary pressure, and to counterbalance the elastic driving forces of lattice. GB motion can be suppressed at temperatures close to the melting point with GB aperture down to 3 nm. In other words, in Schwarz diamond crystals, TPMS GBs remain to be lattice defects highly energetic and intrinsically mobile. SCs including those of lattice structures of other types, point the way for future advances of structurally stable materials.

4.3. Grain boundary relaxation

When GBs are formed between two crystals a considerable variety of modes of relaxations, i.e., the rearrangements of atoms in and near the GB core are possible, depending on GB geometry and the interatomic interactions. The atomic relaxations within and near the GB core often include relaxations that involve the formation of stacking faults in low-stacking-fault energy fcc materials [124]. Recent simulations and experimental investigations indicated that GB structures can be transformed into states with lower excess energy through wiping off extra dislocations, reducing atoms at GB, or atom rearrangement in the GB region, which is summarized as GB relaxation [125,126]. Structurally, Zhou et al. [126] reported that the interaction between partial dislocations and GBs is an effective approach to changes the GB characteristics. As partial dislocations emit from a boundary, the original GB dissociates into two or even three GBs connected by stacking faults, leading to atomic relaxation in GB region and decreasing the GB excess energy. This model of GB relaxation was verified by HRTEM observations in Au [124]. Chen et al. [127] used an in situ ultrahigh-vacuum and HRTEM to observe the electromigration-induced atomic diffusion in the twin-modified GBs. It was revealed that the GB structure is relaxed by interaction with a coherent twin, and the electro-migration induced atomic transport is retarded consequently. The above results imply that GB relaxation can be induced in NS materials by defects reaction.

In the past decades, GB relaxation have been achieved by heat treatment, cyclic loading, ultrasound, etc. [129–131]. These treatments are exterior process without significant microstructural evolutions. Recently, two strategies for inducing GB relaxation have

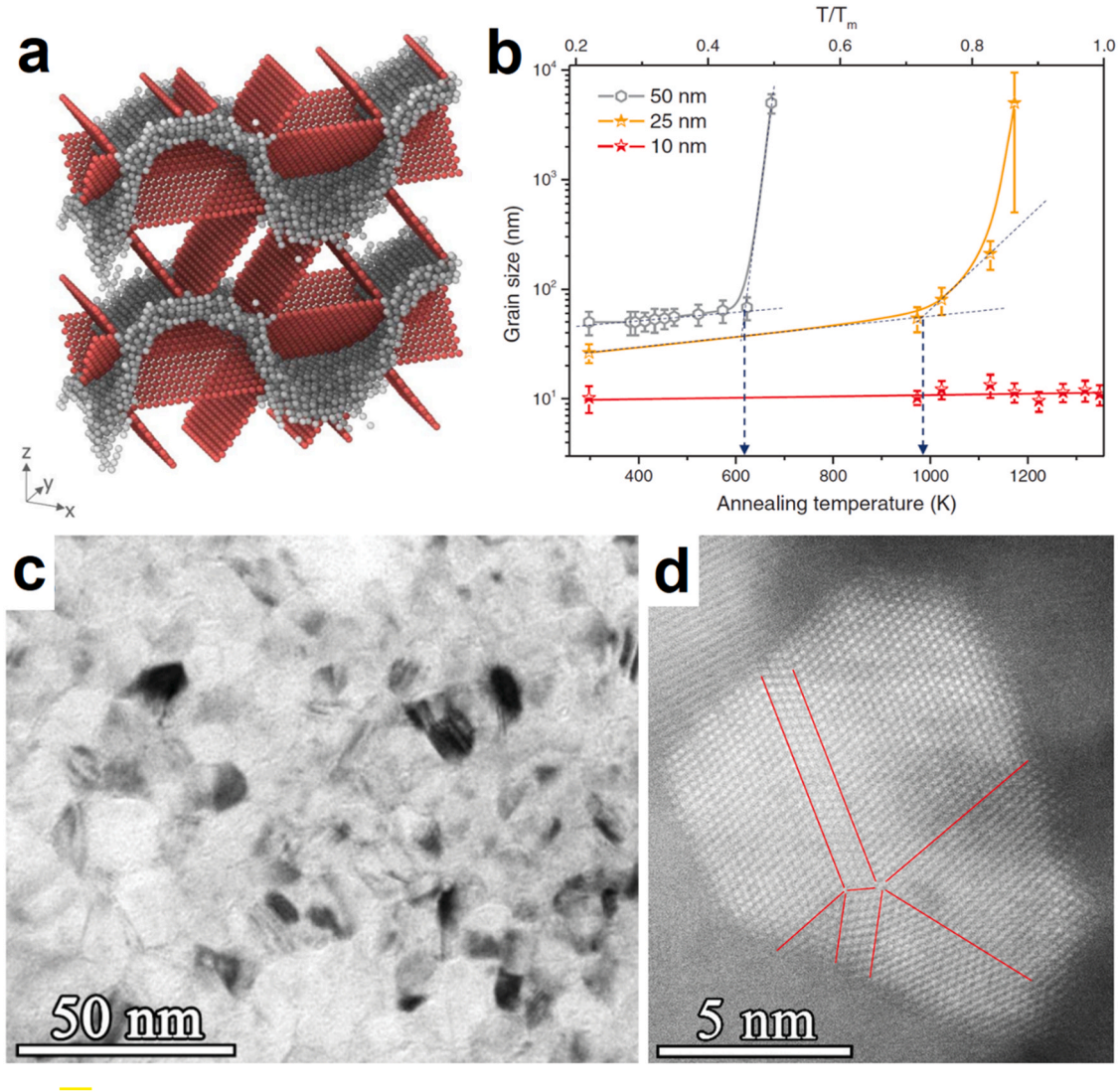

Fig. 13. (a) A section-view of the SC showing Schwarz D-GBs constrained by CTB networks, (b) Grain size variations as a function of annealing temperature for three samples with initial average grain sizes of 50 nm, 25 nm, and 10 nm, respectively, (c) A TEM image of the sample with an initial grain size of 10 nm after annealing at 1348 K for 15 min, the extremely fine grains remained, (d) A HRTEM image of a grain in (B), red lines indicate TBs [121].

been developed in NS pure metals. The first one is to activate partial dislocations by plastic deformation of NG metals below the critical grain sizes [29]. The second is to induce annealing twins by rapid heating the deformed NS metals. Both partial dislocations and annealing twins emitted from GBs and their interactions with GBs induce GB relaxed to low energy states [132]. Zhou et al. [29] reported that plastic deformation can trigger GB relaxation in NG pure Cu and Ni below a critical grain size when the deformation process is dominated by partial dislocation activities. The instability temperature rises substantially at smaller grain sizes, and the nanograins remain stable even above the recrystallization temperatures of coarse grains (usually below 0.4 T_m), as shown in Fig. 14a. An obvious drop in GB energy as grain sizes decreased below ~100 nm (Fig. 14a), meaning a reduced driving force for recrystallization, consistent with the enhanced thermal stability of nanograins below a critical size. Alternatively, a rapidly heated Cu nanograins remain stable at temperatures as high as 0.6 T_m, even higher than the recrystallization temperature of deformed CG Cu [132]. The thermally induced GB relaxation originating from the generation of high-density nanotwins offers an alternative approach to stabilizing NS materials. Fu et al. [128] reported that structural relaxation of GBs breaks the purity-stability dilemma in pure Cu and the thermal stability of NG Cu samples with relaxed GBs, i.e. relaxed NG Cu (RNG), increase with higher purities shown in Fig. 14b. A HRTEM image presented the GB relaxation where high density of twins and stacking faults intersecting with a GB in the relaxed NG-6 N samples in Fig. 14c. Not only pure metals, GB relaxation was founded in alloys such as SMGT processed Inconel 718 nickel-based alloy [133]. Formation of nanolaminated structure with increased fraction of LAGBs provides an alternative way to relax GBs besides activation of partial dislocations in plastic deformation [134].

Actually, GB relaxation is not in the category of structure artifacts, because we cannot define a boundary is a GB relaxed boundary with low-energy state after plastic preparation. Generally, we can

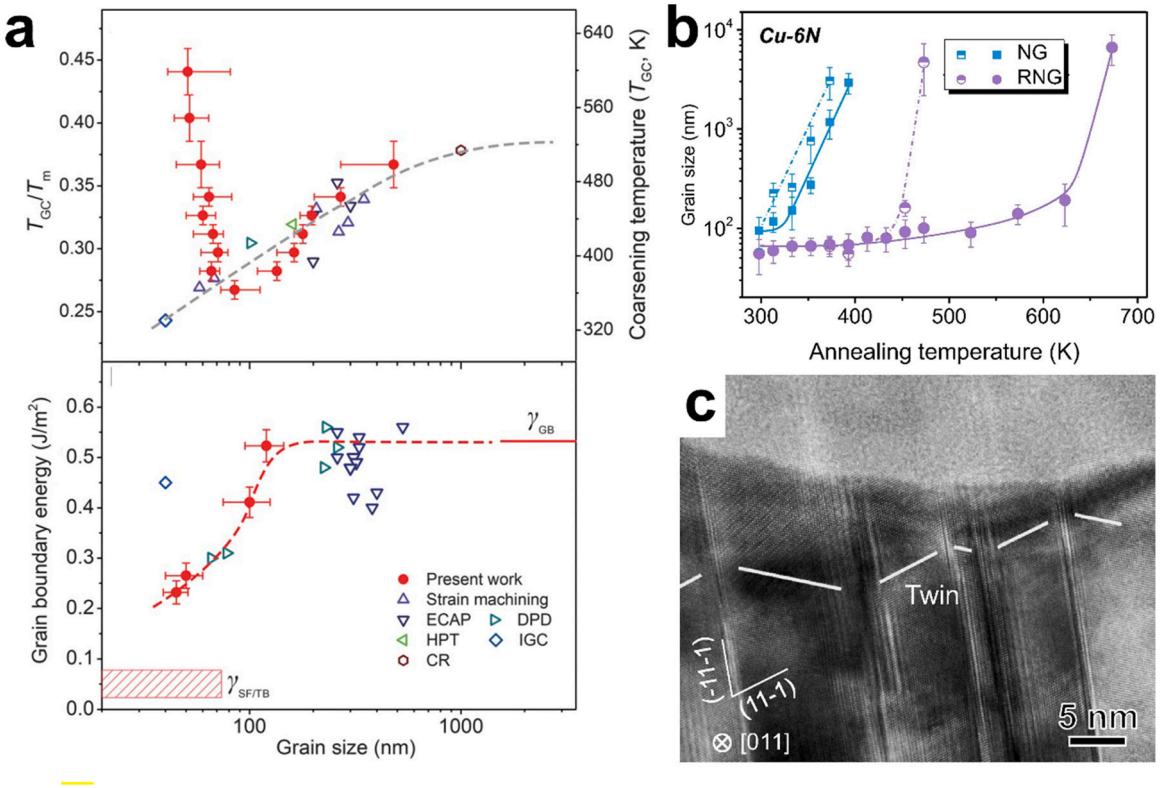

Fig. 14. (a) Grain size dependence of instability temperature and GB energy in Cu, presenting measured grain coarsening (instability) temperature and GB excess energy as a function of average grain size in Cu. Literature data for Cu processed with different techniques are included. Conventional GB energies (γ_{GB}) and energies for stacking faults and TBs ($\gamma_{SF/TB}$) of Cu are indicated [29]. (b) Variations of mean grain size with the annealing temperature for NG-6 N and RNG-6 N samples, respectively. The semi-solid symbols indicate size variations of some nanograins that coarsen firstly and the solid symbols for nanograins with best stability, (c) A HRTEM image showing high density of twins and stacking faults intersecting with a GB in the RNG-6 N samples [128].

only use this thought combined with GB energy measurement to reverse GB relaxation mechanism. But GB relaxation belongs to the scope of structural stability.

5. Conclusions and outlook

In this review, the importance of thermal stability of NS materials and the specific schemes of thermal stability are summarized in detail. Under the premise of alloying elements doping, the thermodynamic and kinetic stabilization approaches have good practicability. Especially with the synergy of the two mechanisms, preeminent thermal stability can be employed in NG materials. It is worth noting that kinetics strategies can stabilize NS metals to higher temperatures than thermodynamic ones. The highlight of this paper is to summarize the microstructural architecture stabilization mechanisms where special low-energy structure or boundaries generate after severe plastic deformation with or without alloying elements. GB relaxation also contributes to the thermal stability by detected low energy and reaction with lattice defects, breaks the purity-stability dilemma in pure metals.

Looking to the future, the following points need to be further studied in thermal stabilization of NS materials. One is large-scaled in situ characterization of microstructural evolution during thermal expose. Due to the limitations of equipment and rigorous experimental environment, most of the microstructural detection are ex situ and more accurate information can be captured with in situ experiments. The second one is more attention should be paid to the synergy or multiple stabilization strategies. Not only combined thermodynamic and kinetic approaches, low-energy microstructure can also be invited to interplay with the two mechanisms. At the meantime, competition and domination between different mechanisms needs to be clarified. The third one is thermal stability of NS materials in the harsh and complex environment, such as ion irradiation, heavy load and high-temperature gases and so on. More unforeseen defects can be introduced in the microstructure and their effect on thermal stability is not clear. The last one is the exploration and promotion of microstructure owing low-energy stable feature. Besides the reaction between defects and GBs, the generation mechanisms of SC and GB relaxation should be studied by atomic experiments. In addition to fcc structured pure Cu and Ni, whether the specific architecture can be produced in other pure metals.

Data availability

No data was used for the research described in the article.

Declaration of Competing Interest

The authors declare that they have no known competing financial interests or personal relationships that could have appeared to influence the work reported in this paper.

Acknowledgments

The authors would like to acknowledge financial supports from the National Natural Science Foundation of China (Grant No. 52105368, 51931003, 51971112 and 51225102), National Key R&D

Program of China (Grant No. 2021YFA1200203), the Fundamental Research Funds for the Central Universities (Grant No. 30919011405) and Nanjing IPE Institute of Green Manufacturing Industry. The authors are thankful for the technical support from Dr. S.F. Li, Jiangsu Key Laboratory of Advanced Micro&Nano Materials and Technology and the Center of Analytical Facilities of Nanjing University of Science and Technology.

References

[1] R.Z. Valiev, Y. Estrin, Z. Horita, T.G. Langdon, M.J. Zehetbauer, Y.T. Zhu, Fundamentals of superior properties in bulk nanoSPD materials, Mater. Res. Lett. 4 (2015) 1–21.
[2] J. Hu, Y.N. Shi, X. Sauvage, G. Sha, K. Lu, Grain boundary stability governs hardening and softening in extremely fine nanograined metals, Science 355 (2017) 1292–1296.
[3] I.A. Ovid'ko, R.Z. Valiev, Y.T. Zhu, Review on superior strength and enhanced ductility of metallic nanomaterials, Prog. Mater. Sci. 94 (2018) 462–540.
[4] Y. Cao, S. Ni, X.Z. Liao, M. Song, Y.T. Zhu, Structural evolutions of metallic materials processed by severe plastic deformation, Mat. Sci. Eng. R. 133 (2018) 1–59.
[5] X.Y. Li, L. Lu, J.G. Li, X. Zhang, H.J. Gao, Mechanical properties and deformation mechanisms of gradient nanostructured metals and alloys, Nat. Rev. Mater. 5 (2020) 706–723.
[6] Z.Y. Zhao, P.K. Bai, R.D.K. Misra, M.Y. Dong, R.G. Guan, Y.J. Li, J.X. Zhang, L. Tan, J.F. Gao, T. Ding, W.B. Du, Z.H. Guo, AlSi10Mg alloy nanocomposites reinforced with aluminum-coated graphene: Selective laser melting, interfacial microstructure and property analysis, J. Alloy. Compd. 792 (2019) 203–214.
[7] X. Chen, Z. Han, X. Li, K. Lu, Lowering coefficient of friction in Cu alloys with stable gradient nanostructures, Sci. Adv. 2 (2016) e1601942.
[8] H.W. Deng, Z.M. Xie, M.M. Wang, Y. Chen, R. Liu, J.F. Yang, T. Zhang, X.P. Wang, Q.F. Fang, C.S. Liu, Y. Xiong, A nanocrystalline AlCoCuNi medium-entropy alloy with high thermal stability via entropy and boundary engineering, Mat. Sci. Eng. a-Struct. 774 (2020) 138925.
[9] T. Chookajorn, H.A. Murdoch, C.A. Schuh, Design of stable nanocrystalline alloys, Science 337 (2012) 951–954.
[10] Q. Huang, D. Yu, B. Xu, W. Hu, Y. Ma, Y. Wang, Z. Zhao, B. Wen, J. He, Z. Liu, Y. Tian, Nanotwinned diamond with unprecedented hardness and stability, Nature 510 (2014) 250–253.
[11] Q. An, W. Yang, B. Liu, S. Zheng, Interface effects on the properties of Cu–Nb nanolayered composites, J. Mater. Res. 35 (2020) 2684–2700.
[12] C. Du, S. Jin, Y. Fang, J. Li, S. Hu, T. Yang, Y. Zhang, J. Huang, G. Sha, Y. Wang, Z. Shang, X. Zhang, B. Sun, S. Xin, T. Shen, Ultrastrong nanocrystalline steel with exceptional thermal stability and radiation tolerance, Nat. Commun. 9 (2018) 5389.
[13] H. Shahmir, M. Nili-Ahmadabadi, A. Shafiee, M. Andrzejczuk, M. Lewandowska, T.G. Langdon, Effect of Ti on phase stability and strengthening mechanisms of a nanocrystalline CoCrFeMnNi high-entropy alloy, Mat. Sci. Eng. a-Struct. 725 (2018) 196–206.
[14] S.L. Xie, Z.B. Wang, K. Lu, Diffusion behavior of Cr in gradient nanolaminated surface layer on an interstitial-free steel, J. Mater. Sci. Technol. 35 (2019) 460–464.
[15] L. Dong, X.F. Xu, B.W. Li, High thermal conductivity and superior thermal stability of amorphous PMDA/ODA nanofiber, Appl. Phys. Lett. 112 (2018) 221904.
[16] M.J.R. Haché, C. Cheng, Y. Zou, Nanostructured high-entropy materials, J. Mater. Res. 35 (2020) 1051–1075.
[17] R.J. Vikram, K. Gupta, S. Suwas, Design of a new cobalt base nano-lamellar eutectic high entropy alloy, Scr. Mater. 202 (2021) 113993.
[18] Z.Y. Li, L.M. Fu, J. Peng, H. Zheng, A.D. Shan, Effect of annealing on microstructure and mechanical properties of an ultrafine-structured Al-containing FeCoCrNiMn high-entropy alloy produced by severe cold rolling, Mat. Sci. Eng. a-Struct. 786 (2020) 139446.
[19] H. Jiang, D.X. Qiao, Y.P. Lu, Z. Ren, Z.Q. Cao, T.M. Wang, T.J. Li, Direct solidification of bulk ultrafine-microstructure eutectic high-entropy alloys with outstanding thermal stability, Scr. Mater. 165 (2019) 145–149.
[20] S. Praveen, J. Basu, S. Kashyap, R.S. Kottada, Exceptional resistance to grain growth in nanocrystalline CoCrFeNi high entropy alloy at high homologous temperatures, J. Alloy. Compd. 662 (2016) 361–367.
[21] M. Annasamy, N. Haghdadi, A. Taylor, P. Hodgson, D. Fabijanic, Static recrystallization and grain growth behaviour of Al0.3CoCrFeNi high entropy alloy, Mat. Sci. Eng. a-Struct. 754 (2019) 282–294.
[22] N.X. Zhou, T. Hu, J.J. Huang, J. Luo, Stabilization of nanocrystalline alloys at high temperatures via utilizing high-entropy grain boundary complexions, Scr. Mater. 124 (2016) 160–163.
[23] R.L. Schoeppner, A.A. Taylor, M.J. Cordill, H.M. Zbib, J. Michler, D.F. Bahr, Precipitate strengthening and thermal stability in three component metallic nanolaminate thin films, Mat. Sci. Eng. a-Struct. 712 (2018) 485–492.
[24] L.F. Zeng, R. Gao, Q.F. Fang, X.P. Wang, Z.M. Xie, S. Miao, T. Hao, T. Zhang, High strength and thermal stability of bulk Cu/Ta nanolamellar multilayers fabricated by cross accumulative roll bonding, Acta Mater. 110 (2016) 341–351.
[25] Y.F. Zhang, R. Su, T.J. Niu, N.A. Richter, S. Xue, Q. Li, J. Ding, B. Yang, H. Wang, X. Zhang, Thermal stability and deformability of annealed nanotwinned Al/Ti multilayers, Scr. Mater. 186 (2020) 219–224.
[26] N.N. Liang, J.Z. Liu, S.C. Lin, Y. Wang, J.T. Wang, Y.H. Zhao, Y.T. Zhu, A multiscale architectured CuCrZr alloy with high strength, electrical conductivity and thermal stability, J. Alloy. Compd. 735 (2018) 1389–1394.
[27] K.A. Darling, A.J. Roberts, Y. Mishin, S.N. Mathaudhu, L.J. Kecskes, Grain size stabilization of nanocrystalline copper at high temperatures by alloying with tantalum, J. Alloy. Compd. 573 (2013) 142–150.
[28] M.A. Atwater, R.O. Scattergood, C.C. Koch, The stabilization of nanocrystalline copper by zirconium, Mater. Sci. Eng. A 559 (2013) 250–256.
[29] X. Zhou, X.Y. Li, K. Lu, Enhanced thermal stability of nanograined metals below a critical grain size, Science 360 (2018) 526–530.
[30] N.N. Liang, Y.H. Zhao, Y. Li, T. Topping, Y.T. Zhu, R.Z. Valiev, E.J. Lavernia, Influence of microstructure on thermal stability of ultrafine-grained Cu processed by equal channel angular pressing, J. Mater. Sci. 53 (2018) 13173–13185.
[31] T. Xiong, S.J. Zheng, Y.T. Zhou, J.C. Pang, Q.Q. Jin, H.L. Ge, X.D. Zheng, L.X. Yang, I.J. Beyerlein, X.L. Ma, Enhancing strength and thermal stability of TWIP steels with a heterogeneous structure, Mat. Sci. Eng. a-Struct. 720 (2018) 231–237.
[32] A.T. Krawczynska, P. Suchecki, B. Adamczyk-Cieslak, B. Romelczyk-Baishya, M. Lewandowska, Influence of high hydrostatic pressure annealing on the recrystallization of nanostructured austenitic stainless steel, Mat. Sci. Eng. a-Struct. 767 (2019) 138381.
[33] A. Duchaussoy, X. Sauvage, K. Edalati, Z. Horita, G. Renou, A. Deschamps, F. De, Geuser, Structure and mechanical behavior of ultrafine-grained aluminum-iron alloy stabilized by nanoscaled intermetallic particles, Acta Mater. 167 (2019) 89–102.
[34] A. Mohammadi, N.A. Enikeev, M.Y. Murashkin, M. Arita, K. Edalati, Developing age-hardenable Al-Zr alloy by ultra-severe plastic deformation: Significance of supersaturation, segregation and precipitation on hardening and electrical conductivity, Acta Mater. 203 (2021) 116503.
[35] A. Dhal, S.K. Panigrahi, M.S. Shunmugam, Insight into the microstructural evolution during cryo-severe plastic deformation and post-deformation annealing of aluminum and its alloys, J. Alloy. Compd. 726 (2017) 1205–1219.
[36] J. Hu, Y.N. Shi, K. Lu, Thermal analysis of electrodeposited nano-grained Ni-Mo alloys, Scr. Mater. 154 (2018) 182–185.
[37] C.J. Marvel, J.A. Smeltzer, B.C. Hornbuckle, K.A. Darling, M.P. Harmer, On the reduction and effect of non-metallic impurities in mechanically alloyed nanocrystalline Ni-W alloys, Acta Mater. 200 (2020) 12–23.
[38] L.L. Tang, Y.H. Zhao, R.K. Islamgaliev, R.Z. Valiev, Y.T. Zhu, Microstructure and thermal stability of nanocrystalline Mg-Gd-Y-Zr alloy processed by high pressure torsion, J. Alloy. Compd. 721 (2017) 577–585.
[39] J. Yi, C.X. Wang, Y.Y. Xia, Comparison of thermal stability between micro- and nano-sized materials for lithium-ion batteries, Electrochem. Commun. 33 (2013) 115–118.
[40] S. Pan, G. Yao, M. Sokoluk, Z. Guan, X. Li, Enhanced thermal stability in Cu-40 wt % Zn/WC nanocomposite, Mater. Des. 180 (2019) 107964.
[41] H.R. Peng, M.M. Gong, Y.Z. Chen, F. Liu, Thermal stability of nanocrystalline materials: thermodynamics and kinetics, Int. Mater. Rev. 62 (2016) 303–333.
[42] R.A. Andrievski, Review Stability of nanostructured materials, J. Mater. Sci. 38 (2003) 1367–1375.
[43] C.C. Koch, R.O. Scattergood, K.A. Darling, J.E. Semones, Stabilization of nanocrystalline grain sizes by solute additions, J. Mater. Sci. 43 (2008) 7264–7272.
[44] C.C. Koch, R.O. Scattergood, M. Saber, H. Kotan, High temperature stabilization of nanocrystalline grain size: Thermodynamic versus kinetic strategies, J. Mater. Res. 28 (2013) 1785–1791.
[45] R.A. Andrievski, Review of thermal stability of nanomaterials, J. Mater. Sci. 49 (2014) 1449–1460.
[46] M. Saber, C.C. Koch, R.O. Scattergood, Thermodynamic grain size stabilization models: an overview, Mater. Res. Lett. 3 (2015) 65–75.
[47] P.C. Millett, R.P. Selvam, A. Saxena, Molecular dynamics simulations of grain size stabilization in nanocrystalline materials by addition of dopants, Acta Mater. 54 (2006) 297–303.
[48] F. Abdeljawad, S.M. Foiles, Stabilization of nanocrystalline alloys via grain boundary segregation: A diffuse interface model, Acta Mater. 101 (2015) 159–171.
[49] X.Y. Song, J.X. Zhang, L.M. Li, K.Y. Yang, G.Q. Liu, Correlation of thermodynamics and grain growth kinetics in nanocrystalline metals, Acta Mater. 54 (2006) 5541–5550.
[50] F.J. Humphreys, M. Hatherly, Recrystallization and Related Annealing Phenomena, Second edition.,, Elsevier,, 2004.
[51] K. Oh-ishi, Z. Horita, D.J. Smith, R.Z. Valiev, M. Nemoto, T.G. Langdon, Fabrication and thermal stability of a nanocrystalline Ni–Al–Cr alloy: Comparison with pure Cu and Ni, J. Mater. Res. 14 (2011) 4200–4207.
[52] K. Lu, Stabilizing nanostructures in metals using grain and twin boundary architectures, Nat. Rev. Mater. 1 (2016) 16019.
[53] V.Y. Gertsman, R. Birringer, On the room-temperature grain growth in nanocrystalline copper, Scr. Metall. Et. Mater. 30 (1994) 577–581.
[54] Y. Huang, S. Sabbaghianrad, A.I. Almazrouee, K.J. Al-Fadhalah, S.N. Alhajeri, T.G. Langdon, The significance of self-annealing at room temperature in high purity copper processed by high-pressure torsion, Mat. Sci. Eng. a-Struct. 656 (2016) 55–66.

[55] M. Ames, J. Markmann, R. Karos, A. Michels, A. Tschope, R. Birringer, Unraveling the nature of room temperature grain growth in nanocrystalline materials, Acta Mater. 56 (2008) 4255–4266.
[56] L. Lu, N.R. Tao, L.B. Wang, B.Z. Ding, K. Lu, Grain growth and strain release in nanocrystalline copper, J. Appl. Phys. 89 (2001) 6408–6414.
[57] K.A. Darling, B.K. VanLeeuwen, C.C. Koch, R.O. Scattergood, Thermal stability of nanocrystalline Fe-Zr alloys, Mater. Sci. Eng. A 527 (2010) 3572–3580.
[58] H.W. Zhang, X. Huang, R. Pippan, N. Hansen, Thermal behavior of Ni (99.967% and 99.5% purity) deformed to an ultra-high strain by high pressure torsion, Acta Mater. 58 (2010) 1698–1707.
[59] G.H. Balbus, J. Kappacher, D.J. Sprouster, F.L. Wang, J. Shin, Y.M. Eggeler, T.J. Rupert, J.R. Trelewicz, D. Kiener, V. Maier-Kiener, D.S. Gianola, Disordered interfaces enable high temperature thermal stability and strength in a nanocrystalline aluminum alloy, Acta Mater. 215 (2021) 116973.
[60] N. Lugo, N. Llorca, J.J. Sunol, J.M. Cabrera, Thermal stability of ultrafine grains size of pure copper obtained by equal-channel angular pressing, J. Mater. Sci. 45 (2010) 2264–2273.
[61] Y.L. Wang, R. Lapovok, J.T. Wang, Y.S. Qi, Y. Estrin, Thermal behavior of copper processed by ECAP with and without back pressure, Mater. Sci. Eng. A 628 (2015) 21–29.
[62] O.F. Higuera-Cobos, J.M. Cabrera, Mechanical, microstructural and electrical evolution of commercially pure copper processed by equal channel angular extrusion, Mater. Sci. Eng. A 571 (2013) 103–114.
[63] Y. Zhang, J.T. Wang, C. Cheng, J.Q. Liu, Stored energy and recrystallization temperature in high purity copper after equal channel angular pressing, J. Mater. Sci. 43 (2008) 7326–7330.
[64] J.D. Schuler, O.K. Donaldson, T.J. Rupert, Amorphous complexions enable a new region of high temperature stability in nanocrystalline Ni-W, Scr. Mater. 154 (2018) 49–53.
[65] N. Zhang, S.B. Jin, G. Sha, J.K. Yu, X.C. Cai, C.C. Du, T.D. Shen, Segregation induced hardening in annealed nanocrystalline Ni-Fe alloy, Mat. Sci. Eng. a-Struct. 735 (2018) 354–360.
[66] T.X. Lu, C.G. Chen, P. Li, C.Z. Zhang, W.H. Han, Y. Zhou, C. Suryanarayana, Z.M. Guo, Enhanced mechanical and electrical properties of in situ synthesized nano-tungsten dispersion-strengthened copper alloy, Mat. Sci. Eng. a-Struct. 799 (2021) 140161.
[67] S. Chakravarty, K. Sikdar, S.S. Singh, D. Roy, C.C. Koch, Grain size stabilization and strengthening of cryomilled nanostructured Cu 12 at% Al alloy, J. Alloy. Compd. 716 (2017) 197–203.
[68] W.J. Lu, C.H. Liebscher, F.K. Yan, X.F. Fang, L.L. Li, J.J. Li, W.Q. Guo, G. Dehm, D. Raabe, Z.M. Li, Interfacial nanophases stabilize nanotwins in high-entropy alloys, Acta Mater. 185 (2020) 218–232.
[69] N. Zhang, D. Gunderov, T.T. Yang, X.C. Cai, P. Jia, T.D. Shen, Influence of alloying elements on the thermal stability of ultra-fine-grained Ni alloys, J. Mater. Sci. 54 (2019) 10506–10515.
[70] Z.B. Jiao, C.A. Schuh, Nanocrystalline Ag-W alloys lose stability upon solute desegregation from grain boundaries, Acta Mater. 161 (2018) 194–206.
[71] C.M. Grigorian, T.J. Rupert, Thick amorphous complexion formation and extreme thermal stability in ternary nanocrystalline Cu-Zr-Hf alloys, Acta Mater. 179 (2019) 172–182.
[72] X.C. Cai, J. Song, T.T. Yang, Q.M. Peng, J.Y. Huang, T.D. Shen, A bulk nanocrystalline Mg–Ti alloy with high thermal stability and strength, Mater. Lett. 210 (2018) 121–123.
[73] B.N. Wang, F. Wang, Z. Wang, L. Zhou, Z. Liu, P.L. Mao, Microstructure and mechanical properties of Mg-Zn-Ca-Zr alloy fabricated by hot extrusion-shearing process, Mat. Sci. Eng. a-Struct. 795 (2020) 139937.
[74] X.C. Cai, B.R. Sun, Y. Liu, N. Zhang, J.H. Zhang, H. Yu, J.Y. Huang, Q.M. Peng, T.D. Shen, Selection of grain-boundary segregation elements for achieving stable and strong nanocrystalline Mg, Mat. Sci. Eng. a-Struct. 717 (2018) 144–153.
[75] G.C. Yao, C.Z. Cao, S.H. Pan, J. Yuan, I. De Rosa, X.C. Li, Thermally stable ultrafine grained copper induced by CrB/CrB2 microparticles with surface nanofeatures via regular casting, J. Mater. Sci. Technol. 58 (2020) 55–62.
[76] L.R. Xiao, Y. Cao, S. Li, H. Zhou, X.L. Ma, L. Mao, X.C. Sha, Q.D. Wang, Y.T. Zhu, X.D. Han, The formation mechanism of a novel interfacial phase with high thermal stability in a Mg-Gd-Y-Ag-Zr alloy, Acta Mater. 162 (2019) 214–225.
[77] G.B. Shan, Y.Z. Chen, M.M. Gong, H. Dong, B. Li, F. Liu, Influence of Al 2 O 3 particle pinning on thermal stability of nanocrystalline Fe, J. Mater. Sci. Technol. 34 (2018) 599–604.
[78] T.J. Niu, Y.F. Zhang, J. Cho, J. Li, H.Y. Wang, X.H. Zhang, Thermal stability of immiscible Cu-Ag/Fe triphase multilayers with triple junctions, Acta Mater. 208 (2021) 116679.
[79] H. Yu, H.P. Zhou, Y. Sun, L.X. Hu, Z.P. Wan, Microstructure thermal stability of nanocrystalline AZ31 magnesium alloy with titanium addition by mechanical milling, J. Alloy. Compd. 722 (2017) 39–47.
[80] Y.P. Wang, R.D. Fu, Y.J. Li, L. Zhao, A high strength and high electrical conductivity Cu-Cr-Zr alloy fabricated by cryogenic friction stir processing and subsequent annealing treatment, Mat. Sci. Eng. a-Struct. 755 (2019) 166–169.
[81] M. Zha, H.-M. Zhang, X.-T. Meng, H.-L. Jia, S.-B. Jin, G. Sha, H.-Y. Wang, Y.-J. Li, H.J. Roven, Stabilizing a severely deformed Al–7Mg alloy with a multimodal grain structure via Mg solute segregation, J. Mater. Sci. Technol. 89 (2021) 141–149.
[82] T. Huang, L. Shuai, A. Wakeel, G. Wu, N. Hansen, X. Huang, Strengthening mechanisms and Hall-Petch stress of ultrafine grained Al-0.3%Cu, Acta Mater. 156 (2018) 369–378.
[83] W. Hanna, K. Maung, M. Enayati, J.C. Earthman, F.A. Mohamed, Grain size stability in a cryomilled nanocrystalline Al alloy powders containing diamantane nanoparticles, Mat. Sci. Eng. a-Struct. 746 (2019) 290–299.
[84] H. Kotan, Thermal stability, phase transformation and hardness of mechanically alloyed nanocrystalline Fe-18Cr-8Ni stainless steel with Zr and Y2O3 additions, J. Alloy. Compd. 749 (2018) 948–954.
[85] A. Devaraj, W. Wang, R. Vemuri, L. Kovarik, X. Jiang, M. Bowden, J.R. Trelewicz, S. Mathaudhu, A. Rohatgi, Grain boundary segregation and intermetallic precipitation in coarsening resistant nanocrystalline aluminum alloys, Acta Mater. 165 (2019) 698–708.
[86] Y.Z. Chen, K. Wang, G.B. Shan, A.V. Ceguerra, L.K. Huang, H. Dong, L.F. Cao, S.P. Ringer, F. Liu, Grain size stabilization of mechanically alloyed nanocrystalline Fe-Zr alloys by forming highly dispersed coherent Fe-Zr-O nanoclusters, Acta Mater. 158 (2018) 340–353.
[87] X.B. Feng, J.Y. Zhang, Z.R. Xia, W. Fu, K. Wu, G. Liu, J. Sun, Stable nanocrystalline NbMoTaW high entropy alloy thin films with excellent mechanical and electrical properties, Mater. Lett. 210 (2018) 84–87.
[88] A. Ahadi, A.R. Kalidindi, J. Sakurai, Y. Matsushita, K. Tsuchiya, C.A. Schuh, The role of W on the thermal stability of nanocrystalline NiTiWx thin films, Acta Mater. 142 (2018) 181–192.
[89] S.A. Kube, W.Y. Xing, A. Kalidindi, S. Sohn, A. Datye, D. Amram, C.A. Schuh, J. Schroers, Combinatorial study of thermal stability in ternary nanocrystalline alloys, Acta Mater. 188 (2020) 40–48.
[90] H. Wang, W. Song, M. Liu, S. Zhang, L. Ren, D. Qiu, X.Q. Chen, K. Yang, Manufacture-friendly nanostructured metals stabilized by dual-phase honeycomb shell, Nat. Commun. 13 (2022) 2034.
[91] G.B. Shan, Y.Z. Chen, Y.J. Li, C.Y. Zhang, H. Dong, Y.B. Cong, W.X. Zhang, L.K. Huang, T. Suo, F. Liu, High temperature creep resistance of a thermally stable nanocrystalline Fe-5 at% Zr steel, Scr. Mater. 179 (2020) 1–5.
[92] J.S. Riano, A.M. Hodge, Exploring the thermal stability of a bimodal nanoscale multilayered system, Scr. Mater. 166 (2019) 19–23.
[93] B.Q. Wei, W.Q. Wu, D.Y. Xie, M. Nastasi, J. Wang, Strength, plasticity, thermal stability and strain rate sensitivity of nanograined nickel with amorphous ceramic grain boundaries, Acta Mater. 212 (2021) 116918.
[94] Q. Li, J. Cho, S.C. Xue, X. Sun, Y.F. Zhang, Z.X. Shang, H.Y. Wang, X.H. Zhang, High temperature thermal and mechanical stability of high-strength nanotwinned Al alloys, Acta Mater. 165 (2019) 142–152.
[95] J. Gao, S. Jiang, H. Zhang, Y. Huang, D. Guan, Y. Xu, S. Guan, L.A. Bendersky, A.V. Davydov, Y. Wu, H. Zhu, Y. Wang, Z. Lu, W.M. Rainforth, Facile route to bulk ultrafine-grain steels for high strength and ductility, Nature 590 (2021) 262–267.
[96] Z. Wang, Z. Chen, Y. Fan, J. Shi, Y. Liu, X. Shi, J. Xu, Thermal stability of the multicomponent nanocrystalline Ni–ZrNbMoTa alloy, J. Alloy. Compd. 862 (2021) 158326.
[97] P. Zheng, Y. Li, J. Zhang, J. Shen, T. Nagasaka, T. Muroga, H. Abe, On the thermal stability of a 9Cr-ODS steel aged at 700 °C up to 10000h - Mechanical properties and microstructure, Mater. Sci. Eng.: A 783 (2020) 139292.
[98] J. Esquivel, M.G. Wachowiak, S.P. O'Brien, R.K. Gupta, Thermal stability of nanocrystalline Al-5at%Ni and Al-5at%V alloys produced by high-energy ball milling, J. Alloy. Compd. 744 (2018) 651–657.
[99] C.S. Smith, Grains, phases, and interfaces: an interpretation of microstructure (reprinted), Met. Mater. Trans. A 41A (2010) 1064–1100.
[100] P.A. Manohar, M. Ferry, T. Chandra, Five decades of the zener equation, ISIJ Int. 38 (1998) 913–924.
[101] F.L. Wang, Y.P. Li, X.D. Xu, Y. Koizumi, K. Yamanaka, H.K. Bian, A. Chiba, Superthermostability of nanoscale TIC-reinforced copper alloys manufactured by a two-step ball-milling process, Philos. Mag. 95 (2015) 4035–4053.
[102] F.J. Humphreys, A unified theory of recovery, recrystallization and grain growth, based on the stability and growth of cellular microstructures—II. The effect of second-phase particles, Acta Mater. 45 (1997) 5031–5039.
[103] Z.Z. Li, S.T. Zhao, R.O. Ritchie, M.A. Meyers, Mechanical properties of high-entropy alloys with emphasis on face-centered cubic alloys, Prog. Mater. Sci. 102 (2019) 296–345.
[104] X.Z. Gao, Y.P. Lu, B. Zhang, N.N. Liang, G.Z. Wu, G. Sha, J.Z. Liu, Y.H. Zhao, Microstructural origins of high strength and high ductility in an AlCoCrFeNi2.1 eutectic high-entropy alloy, Acta Mater. 141 (2017) 59–66.
[105] Y.Y. Zhao, H.W. Chen, Z.P. Lu, T.G. Nieh, Thermal stability and coarsening of coherent particles in a precipitation-hardened (NiCoFeCr)94Ti2Al4 high-entropy alloy, Acta Mater. 147 (2018) 184–194.
[106] N. Liang, R. Xu, G. Wu, X. Gao, Y. Zhao, High thermal stability of nanocrystalline FeNi2CoMo0.2V0.5 high-entropy alloy by twin boundary and sluggish diffusion, Mat. Sci. Eng. a-Struct. 848 (2022) 143399.
[107] H. Guo, F.W. Tang, Y. Liu, Z. Zhao, H. Lu, C. Hou, X.Y. Song, Thermal stability of phase-separated nanograin structure during heat treatment, J. Alloy. Compd. 875 (2021) 160055.
[108] K.A. Darling, M.A. Tschopp, B.K. VanLeeuwen, M.A. Atwater, Z.K. Liu, Mitigating grain growth in binary nanocrystalline alloys through solute selection based on thermodynamic stability maps, Comput. Mater. Sci. 84 (2014) 255–266.
[109] P. Wynblatt, D. Chatain, Y. Pang, Some aspects of the anisotropy of grain boundary segregation and wetting, J. Mater. Sci. 41 (2006) 7760–7768.

[110] A.R. Kalidindi, T. Chookajorn, C.A. Schuh, Nanocrystalline materials at equilibrium: a thermodynamic review, Jom-Us 67 (2015) 2834–2843.
[111] W.T. Xing, A.R. Kalidindi, D. Amram, C.A. Schuh, Solute interaction effects on grain boundary segregation in ternary alloys, Acta Mater. 161 (2018) 285–294.
[112] M. Wagih, C.A. Schuh, Thermodynamics and design of nanocrystalline alloys using grain boundary segregation spectra, Acta Mater. 217 (2021) 117177.
[113] D. Amram, C.A. Schuh, Interplay between thermodynamic and kinetic stabilization mechanisms in nanocrystalline Fe-Mg alloys, Acta Mater. 144 (2018) 447–458.
[114] B.G. Clark, K. Hattar, M.T. Marshall, T. Chookajorn, B.L. Boyce, C.A. Schuh, Thermal Stability Comparison of Nanocrystalline Fe-Based Binary Alloy Pairs, Jom-Us 68 (2016) 1625–1633.
[115] R. Kirchheim, Grain coarsening inhibited by solute segregation, Acta Mater. 50 (2002) 413–419.
[116] H.R. Peng, B.S. Liu, F. Liu, A strategy for designing stable nanocrystalline alloys by thermo-kinetic synergy, J. Mater. Sci. Technol. 43 (2020) 21–31.
[117] L.X. Sun, N.R. Tao, K. Lu, A high strength and high electrical conductivity bulk CuCrZr alloy with nanotwins, Scr. Mater. 99 (2015) 73–76.
[118] X.C. Liu, H.W. Zhang, K. Lu, Strain-induced ultrahard and ultrastable nanolaminated structure in nickel, Science 342 (2013) 337–340.
[119] B.B. Zhang, N.R. Tao, K. Lu, A high strength and high electrical conductivity bulk Cu-Ag alloy strengthened with nanotwins, Scr. Mater. 129 (2017) 39–43.
[120] A. Dhal, B. Prathyusha, R. Kumar, S.K. Panigrahi, Twin evolution and work-hardening phenomenon of a bulk ultrafine grained copper with high thermal stability and strength-ductility synergy, Mat. Sci. Eng. a-Struct. 802 (2021) 140622.
[121] X.Y. Li, Z.H. Jin, X. Zhou, K. Lu, Constrained minimal-interface structures in polycrystalline copper with extremely fine grains, Science 370 (2020) 831–836.
[122] Z. Jin, X. Li, K. Lu, Formation of Stable Schwarz Crystals in Polycrystalline Copper at the Grain Size Limit, Phys. Rev. Lett. 127 (2021) 136101.
[123] W. Xu, B. Zhang, X.Y. Li, K. Lu, Suppressing atomic diffusion with the Schwarz crystal structure in supersaturated Al-Mg alloys, Science 373 (2021) 683–687.
[124] K.L. Merkle, Atomic-scale grain boundary relaxation modes in metals and ceramics, Microsc. Microanal. 3 (2003) 339–351.
[125] A.A. Nazarov, Nonequilibrium grain boundaries in bulk nanostructured metals and their recovery under the influences of heating and cyclic deformation. Review, Lett. Mater. 8 (2018) 372–381.
[126] X. Zhou, X.Y. Li, K. Lu, Stabilizing nanograins in metals with grain boundary relaxation, Scr. Mater. 187 (2020) 345–349.
[127] K.C. Chen, W.W. Wu, C.N. Liao, L.J. Chen, K.N. Tu, Observation of atomic diffusion at twin-modified grain boundaries in copper, Science 321 (2008) 1066–1069.
[128] H. Fu, X. Zhou, H. Xue, X. Li, K. Lu, Breaking the purity-stability dilemma in pure Cu with grain boundary relaxation, Mater. Today 55 (2022) 66–73.
[129] D. Jang, M. Atzmon, Grain-boundary relaxation and its effect on plasticity in nanocrystalline Fe, J. Appl. Phys. 99 (2006) 083504.
[130] R.T. Murzaev, D.V. Bachurin, A.A. Nazarov, Relaxation of the residual defect structure in deformed polycrystals under ultrasonic action, Phys. Met. Metallogr. 118 (2016) 621–629.
[131] T.J. Rupert, C.A. Schuh, Mechanically driven grain boundary relaxation: a mechanism for cyclic hardening in nanocrystalline Ni, Philos. Mag. Lett. 92 (2012) 20–28.
[132] X.Y. Li, X. Zhou, K. Lu, , Rapid heating induced ultrahigh stability of nanograined copper, Sci. Adv. 6 (2020) eaaz8003.
[133] J. Ding, Y. Zhang, T. Niu, Z. Shang, S. Xue, B. Yang, J. Li, H. Wang, X. Zhang, Thermal stability of nanocrystalline gradient inconel 718 alloy, Crystals 11 (2021) 53.
[134] J. Hou, X. Li, K. Lu, Formation of nanolaminated structure with enhanced thermal stability in copper, Nanomater. (Basel) 11 (2021) 2252.